(26) Larson, R. G. *Rheol. Acta* **1985**, *24*, 327.
(27) Kiss, G.; Porter, R. S. *J. Polym. Sci., Polym. Symp.* **1978**, *65*, 193.
(28) Venkatraman, S.; Berry, G. C.; Einaga, Y. *J. Polym. Sci., Polym. Phys. Ed.* **1985**, *23*, 1275.
(29) Frost, R. S.; Flory, P. J. *Macromolecules* **1978**, *11*, 1134.
(30) Lekkerkerker, H. N. W.; Coulon, P.; van der Haegen, R.; Deblieck, R.; *J. Chem. Phys.* **1984**, *80*, 3427.
(31) Marrucci, G.; Grizzuti, N. *J. Non.-Newtonian Fluid Mech.* **1984**, *14*, 103.

Fractal Nature of One-Step Highly Branched Rigid Rodlike Macromolecules and Their Gelled-Network Progenies

S. M. Aharoni*

Polymer Science Laboratory, Allied-Signal Research and Technology, Allied-Signal Inc., P.O. Box 1087R, Morristown, New Jersey 07962

N. S. Murthy and K. Zero

Analytical Sciences Laboratory, Allied-Signal Research and Technology, Allied-Signal Inc., Morristown, New Jersey 07962

S. F. Edwards

Cavendish Laboratory, Cambridge University, Madingley Road, Cambridge CB3 0HE, U.K.
Received September 14, 1989; Revised Manuscript Received November 20, 1989

ABSTRACT: Several highly branched polymeric systems were prepared by a one-step polymerization. They are characterized by stiff trifunctional branchpoints connected by rigid rodlike segments. A few systems with flexible segments were prepared for comparison. The systems were studied in their pregel and postgel states. Small-angle X-ray scattering intensity measurements from bone-dry and concentrated solutions are consistent with the expectations of the polymeric fractal model. Static light scattering combined with photon correlation spectroscopy revealed the polymeric species in the pregel state to be highly branched. End-group titration and segment-tip decoration by iodine clearly indicate the highly branched nature of the pregel as well as postgel systems. The kinetics of particle growth prior to the gel point and solution property characteristics both agree with the fractal model. Scanning electron microscopy of the dried pregel material yielded typical fractal morphology. Porosimetry studies of one dry postgel network supports the fractal concept. When compatible macromolecular fillers were added to the reaction mixture of the one-step systems prior to the gel point, the modulus of the resulting "infinite" network gels was consistently lower than the modulus of the corresponding neat gel. When the rigid networks were prepared in two steps from preexisting high-M chains, their modulus increased upon the addition of the same filler macromolcules. The weakening effect of filler macromolecules was even more dramatic in the case of one-step flexible polymer gels. When short, monodisperse oligomers were added to the one-step rigid networks instead of their long filler analogues, no effect on the modulus was observed. We propose two growth morphologies to explain our observations. In the one-step polymerization, random nucleations form polymer fractals. They cluster together and when a sufficient number of them grow enough, a contiguous network is formed that, when reaching from one end of the sample to the other, is best described as an "infinite" cluster of polymeric fractals. At this point gelation occurs. Further reaction more or less fills the sample volume with additional fractals, which may or may not be covalently attached to the "infinite" network. The filler macromolecules are pushed ahead of the fractal growth fronts until trapped in between. Thus they reduce the concentration of strong bonds between fractals and clusters causing a reduction of the modulus of the ensemble as a whole. The oligomers are shorter than the network's segments, so they can be accommodated within the growing fractal and not affect the modulus of the gelled network. In the case of two-step network formation, the solution is randomly filled with high-M macromolecules and when these cross-link the system rapidly gels with only minor variations in local cross-link concentration. Long filler macromolecules appear not to measurably interfere with the formation of interchain bonds. Hence, the modulus of the network does not decrease.

Introduction

Until recently, most theoretical treatments studied covalent polymeric networks that consist of flexible Gaussian segments cross-linked by residues of fully reacted functionalities.[1,2] The mathematics of the standard approach was in the spirit of the mean-field theory. The material was considered essentially homogeneous with cross-links uniformly arranged through it (physical assumption) and the closed loops and other imperfections treated as perturbations (a mathematical assumption). Moreover, polymer chemistry provided networks of short monomers and flexible long segments. All these conditions can be changed through the introduction of rigid segments interconnected at stiff or flexible branchpoints, and the corresponding mathematics has to respond. Thus, the basic papers[3-8] have to be modified when rigid rodlike polymers comprise the network rather than flexible ones. In their unbranched and un-cross-linked form, these rodlike polymers are liquid crystalline in nature.

There are three fundamentally different methods of preparing gelled, covalently linked polymeric networks. One is to start with a solution of the appropriate monomers, whose average functionality is higher than 2.0, and conduct the polymerization in a single step. This procedure will be called here a one-step method. The growing polymeric entities are highly branched and, as will

0024-9297/90/2223-2533$02.50/0

be demonstrated below, conform to the polymeric fractal model. When the total polymer concentration in the reaction mixture, C_0, is above a certain critical threshold, C^*_0, the system eventually solidifies and a gel is formed. The second method requires the preparation of high molecular weight (high-M) polymeric chains in a first step and then cross-linking them many times along the chains in a second, separate step. This will be called a two-step method. The cross-linking may be done by irradiation, which will not be considered in this work, or by the use of a suitable cross-linking agent at an appropriate concentration in solution. The third method is similar to the two-step method, except that the cross-linking takes place exclusively at the reactive chain ends. In this work, chain end-linked systems will not be dealt with. The one-step and two-step methods are expected to produce two different kinds of molecular networks[9] and also to be different from the third kind of network, constructed from long flexible chains end-linked by polyfunctional junction points.

The condensation-type cross-linking process described in this paper for the creation of one-step networks of rigid members must start at random cross-link centers, or nuclei, and then grow by an aggregation process until a complete gelled network is formed. The classic vulcanization of rubber has, of course, elements of this problem, since it is well-known that the existence of one cross-link encourages (by enhancing proximity and slowing down chain motion) the formation of another in its neighborhood. However, in the case of flexible chains, it is believed that this effect does not materially change the simple theory; here it does. The formation of "gel" around cross-link centers by aggregation leads one to the theory of aggregation that gives rise to power laws associated with fractal structures. Such fractals have special elastic properties[10–15] but eventually interpenetrate and link up, so that the purity of the fractal concept fades.

The resultant rigid segment network gels are in marked contrast with the classical gels. A classical network gel is like a solution or melt with cross-links acting as a blockage to the slow flow of the material, i.e., creating a nonvanishing modulus at zero frequency. The frequency-dependent complex modulus of a melt is reasonably well understood[16] in terms of the picture of one flexible polymer chain enclosed by the other chains in an effective tube of radius $a \gg b$, the Kuhn segment length of the chain. Under these circumstances, the shear properties of the material are dominated by entropy, i.e., by the movement of the polymer in the tube (and for un-cross-linked material, by its escape from an original tube to create a new one in the reptation process; but this will not arise here). The gelled networks created in this work are quite different. One can visualize a situation where $b \gg a$ and where the entropic contributions can be small compared to the simple energy of bending the chains. One can see that all conditions between the two extremes are possible, and a wide new world of materials begins to emerge.

Fractals are self-similar. That is, the same properties are found at each length scale, and a power law governs the relationship between mass and size.[17] In each such structure, the concentration of polymeric material gradually decreases as a function of distance from the center. The average diameter and number of such polymeric fractals continue to grow until all reactive monomeric species are consumed when polymerization is carried out in dilute solutions or, in the case of higher concentrations, until the fractals impinge upon one another and gelation takes place. At gelation some covalent bonds between contiguous fractals are undoubtedly formed, but other interactions, such as hydrogen bonds between polyamide chains, can form the gel on their own. The concentration of covalent bonds at the interfacial layer is expected to be lower than in the fractals' cores, especially in the case of rigid rodlike fractals. The polymerization reaction continues beyond the gel point with the concomitant creation of additional covalent bonds between fractals and the probable formation of additional fractals. Stiff polymeric fractals growing in solution, having rodlike segments between stiff branchpoints, are likely to enhance the above because of the overall stiffness of the fractal and because the growing rodlike segments cannot easily bend or twist to adopt the appropriate angle for reaction with approaching monomeric species or for intrafractal cyclization.

Since they consist of long polymeric chains cross-linked at regular intervals or at random along the backbone with many other such chains present in solution, the gelled two-step networks may not behave as fractals at all but may be closer in shape to sheaves of macromolecules held together by interchain cross-links. The sheaflike appearance is expected to be more accentuated in the case of rodlike macromolecules and gradually approach fringed-micelle behavior as the initial chains turn more and more flexible. If such a system can be called fractal at all, then its fractals will be very large in size and rather diffuse with probably close to uniform polymer concentration throughout.

In this work we deal exclusively with covalent polymeric gels, that is, covalently cross-linked polymeric networks prepared by polycondensation and equilibrated in solution. We limit ourselves almost exclusively to polymer concentrations in the gels of 10% or less. The emphasis is on rigid rodlike networks, where the branchpoints are stiff and the segments between them are rigid, with a few flexible segment networks used for comparison. The descriptive term "rigid rodlike" is correctly applied to polymers such as aromatic polyimides or para-substituted polybenzoxazoles. Here, however, we elected to be consistent with our previous work[18–20] and follow tradition by describing the nature of our para-substituted polyamide segments as rigid rodlike.

We shall show that the nature of the growing one-step rigid aggregates in the pregel state is consistent with the fractal model. It will also be demonstrated that because of the branchpoint and segmental rigidity and the rather large average length of the segments between branchpoints, the rigid one-step fractals are remarkably porous on the scale of solvent molecules. We shall further show that differences in the growth nature of one-step and two-step rigid systems are reflected in differences in the behavior of the gels of corresponding "infinite" networks. This will be done by the introduction of un-cross-linkable macromolecular fillers into the evolving gelled network during the process of their formation. These fillers are highly soluble in the reaction medium and compatible with the cross-linked networks in the gels. The idea is that in the one-step network formation the filler macromolecules may interfere with the intermeshing of the impinging fractals and with the formation of covalent bonds between them, reducing the expected modulus of the gelled networks containing the filler macromolecules. In the sheaflike two-step gels, on the other hand, the presence of filler macromolecules is not significantly detrimental to the cross-linking of the other high-M chains and the formation of networks. Hence, the presence of compatible filler macromolecules in the two-step gels is expected to increase the modulus as compared with the neat networks.

Experimental Section

Rigid rodlike gelled networks and flexible gelled networks were prepared by the Yamazaki procedure[21] as modified by Aharoni for the preparation of cross-linked systems.[18-20] Besides the solvent mixture, *N*,*N*-dimethylacetamide (DMAc) containing 5 wt % anhydrous LiCl, and the appropriate monomer composition, the reaction mixture contained a slight molar excess of pyridine and triphenyl phosphite (TPP). When macromolecular or oligomeric filler was incorporated into the evolving gels, the requisite amount of such macromolecules was dissolved in the solvent mixture prior to the addition of the other ingredients. The preparation of most gelled networks in this study was conducted at 112 ± 1 °C, and the reaction was allowed to proceed for exactly 3 h after each system reached its gel point. In a study of the critical concentration for gelation, C^*_0, the reaction was allowed to continue for 3 h from the addition of TPP for systems too dilute to gel or for 3 h after gelation for the more concentrated ones. Filler macromolecules were prepared from the appropriate monomers by the Yamazaki procedure, at 105–115 °C, at monomer concentration, C_0, of 10%. Here the reactions were allowed to continue for 3 h after a significant increase in solution viscosity was evident. Identical conditions were used for the preparation of the monodisperse oligomeric filler, branched systems in their pregel and, on occasion, postgel state. In several series aliquots were withdrawn from the reaction mixtures until the gel point was reached. Each aliquot was rapidly quenched in methanol, carefully washed, dried, and characterized. The purified product of one series (59E) was subsequently used to study its ability to form an "infinite" network gel in the absence of monomers and for the purpose of decorating the segment tips with iodinated groups. Kinetic studies were performed by conducting the polycondensation reaction with the oscillating sphere of a Nametre direct readout viscometer immersed in the reaction mixture. In order to minimize data scatter, each given type of measurement was conducted, as much as possible, on members of the same series.

Schotten-Baumann-type reactions were employed to prepare a tetrafunctional monomer for one of the filler macromolecules and for the preparation of two high-M polyamide chains capable of undergoing subsequent cross-linking by the Yamazaki procedure. Except for the tetrafunctional filler macromolecule, all branchpoints in this study were trifunctional.

After synthesis, the gelled networks were cut into slabs with a sharp blade. Their modulus was measured at ambient temperature (ca. 20 °C) without immersion in solvent. When immersed in solvent and immediately measured, the modulus was no different from that of the unimmersed slabs, within the experimental error margin of our measurements. When equilibrated in DMAc, a process that took several weeks and required several solvent exchanges, the gels swelled to different degrees relative to the as-prepared ones. The modulus measured on the swelled gels was lower than the one obtained from the corresponding as-prepared gels and, again, was insensitive to whether the specimens were immersed in DMAc during measurements or not. The equilibrum modulus, G, was determined from the depth of penetration of a flat surface into the gel under four different loads. The penetration depth was measured by a Humboldt universal penetrometer equipped with a flat penetrating tip whose surface area was changed such that the depth of penetration was limited to fractions of a millimeter. Details of the measurements are given in a previous paper by Aharoni and Edwards.[20] Sol–gel fractionation was conducted in a routine manner as described in ref 20.

Dilute solution viscosity of the soluble fractions was measured in DMAc/5% LiCl at 20 °C with a Nametre direct readout viscometer and at 25 °C in internal dilution Cannon-Ubbelohde glass viscometers with solvent efflux times longer than 100 s. Concentrated solution viscosity was measured at 20 °C in the Nametre viscometer.

The weight-average molecular weight, M_w, of pregel samples was measured on their solutions in DMAc/5% LiCl in a low-angle laser light scattering Chromatix KMX-6 instrument. The hydrodynamic radius, R_H, and molecular weight distributions in terms of M_w/M_n and M_z/M_w were determined from diffusion measurements in a Langley-Ford LSA-II photon correlation spectrometer (PCS). The molecular weight ratios were determined from the distributions of the PCS data. Prior to measurement, all solutions were filtered through Millipore filters with 0.2 μm pore size. In order to observe the size-independent power-law scattering behavior for a fractal, one requires that $R \gg 1/q$, where R is the radius of the fractal and q is the scattering vector defined below. For visible light, $1/q > 200$ Å. Consequently, our polymers were much too small to exhibit this scattering behavior by the use of the light scattering.

Scanning electron microscope (SEM) micrographs were obtained from gold-sputtered samples by using Hitachi S570 SEM. Densities were measured by pycnometry in mixtures of chlorinated solvents with hexanes or methanol. None of these mixtures is a solvent or swelling agent for our polymers. Some additional measurements on the dried gelled network were conducted by helium pycnometry and mercury porosimetry by means of a Micromeritics Auto-Pore 9200 instrument.

Wide-angle X-ray diffraction (WAXD) patterns were obtained from the postgel networks and the pregel molecular aggregates in their bone-dry and solvent-swollen states. For the purpose of swelling, DMAc/5% LiCl was used. The patterns were obtained in a Philips APD 3600 automatic diffractometer operating in the parafocus mode with monochromatized Cu Kα radiation. After background subtraction, crystallinity indices were obtained from the diffraction patterns as is common in the art. Small-angle X-ray scattering (SAXS) data were collected from samples in 1.5-mm diameter quartz capillaries. The patterns were recorded with nickel-filtered copper radiation on a Franks camera using a position-sensitive proportional counter controlled by an IBM PC/AT computer. Pinhole collimation was obtained by using a pair of delimiting slits at right angles to the single focusing mirror. The distance of the sample to detector window was 325 mm and was filled with helium. Data were collected from 1 to 16 h, depending on the absorption and scattering intensity of each sample. The data were corrected for absorption by measuring the attenuation of the 50.3-Å reflection from lead stearate. The background due to a blank capillary and due to the solvent were subtracted, respectively, from the bone-dry powder and pastelike solution data. For the purpose of measuring the scattered intensity $I(q)$ as a function of the momentum transfer q, data were collected over the range of $10^{-1.8}$ Å$^{-1} < q < 10^{-0.8}$ Å^{-1}. For segmental length l_0 of 38.5 Å, this translates to $0.61 < ql_0 < 6.10$. The momentum transfer q is also called the scattering vector and is defined[22] as

$$q = 4\pi \sin(\theta/2)\lambda \tag{1}$$

in terms of the scattering angle θ and the wavelength λ of the scattered beam. When the scattering angle is small, as is true in most SAXS experiments, the above may be approximated[23] by

$$q = 2\pi\theta/\lambda \tag{2}$$

but in this work only relationship (1) was used.

The structures and purity of the monomers and pregel polymers were confirmed by ^{13}C NMR spectra obtained with a Varian XL-200 Fourier-transform NMR spectrometer from solutions in deuteriated DMAc or Me_2SO. Infrared (IR) procedures were used to obtain a qualitative estimate of the relative amounts of "free" and H-bonded amide groups in bone-dry samples of one-step rigid networks and the chemically similar linear rigid filler macromolecules. Amide groups that are not hydrogen bonded are associated with an IR envelope centered around 3400 cm^{-1}, while H-bonded aromatic amides produce an envelope at about 3350–3300 cm^{-1}. A qualitative estimate of the amount of "free" amide amide groups can be gathered from evaluation of the areas under both IR envelopes. The spectra were obtained by using a Perkin-Elmer Model 983 ratio-recording double-beam infrared spectrophotometer under 3 cm^{-1} at 100-cm^{-1} resolution conditions. The samples were ground with KBr powder, pelletized under 9-ton ram pressure, predried by using flowing liquid nitrogen boiloff, then dried at 100 °C under 220 Torr for 16 h, and finally transferred hot to a flowing nitrogen dry instrument to cool. Samples prepared in this fashion will be called "bone-dry" samples.

End-group titrations were conducted in the following manner: 3.00 g of each sample was dissolved with warming in 60 mL of DMAc/5% LiCl. After full dissolution and uniformity were achieved, the samples were cooled to ambient tempera-

ture. The titrations were carried out by first titrating against aqueous NaOH (0.2094 N) and then back-titrating with aqueous HCl (0.2378 N). The total volumes of base and acid were on the order of 20–30 mL per sample. As a consequence, some polymer precipitated out during the titration and had to be constantly cleaned off the calomel electrode. The pH values were recorded after each milliliter of added titrant and the results plotted. From the breaks in the curves, the weights per mole of carboxylic acid and amino end groups in each sample were calculated. Iodine analysis was performed by common analytical procedures.

The monomer 4,4′-diaminobenzanilide (DABA) was obtained from Sandoz Corp. The monomer bis(*p*-aminobenzoate) trimethylene glycol (BABTMG) was obtained from Polaroid Corp. under the trade name Polacure 740M. Both were recrystallized from methanol prior to use. A 36 carbon atom dimer acid (Empol 1010) was obtained from Emery Industries. All other starting materials, reagents, and solvents were obtained from chemical supply houses in the highest available purity and used as received.

Results

(a) Systems for Pregel, Growth Kinetics, and Critical Concentration for Gelation Studies. For the purpose of studying the growth kinetics of one-step highly branched systems, a series (series 37) of highly branched polyamides was prepared in which all branchpoints are stiff. The monomers for the trifunctional branchpoints were either 1,3,5-benzenetricarboxylic acid (BTCA) or tris(*p*-carboxyphenyl)-1,3,5-benzenetriamide (TCPBT),

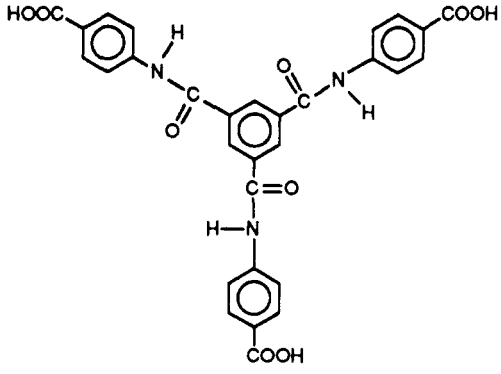

I

which was prepared by us in a Schotten-Baumann-type procedure from *p*-aminobenzoic acid and 1,3,5-benzenetricarboxylic acid chloride. The reaction of BTCA with DABA in 2:3 molar ratio produced a network with rigid rodlike segments of length l_0 = 19.5 Å

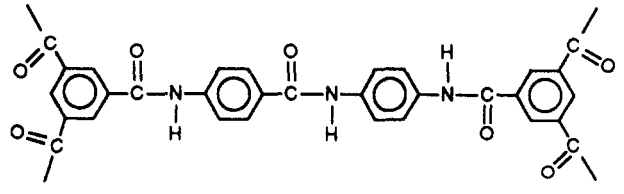

II

and the reaction of 2:3 molar ratio TCPBT with DABA resulted in a network where all segments are rigid and of identical length, l_0 = 32.5 Å. They appear as III.

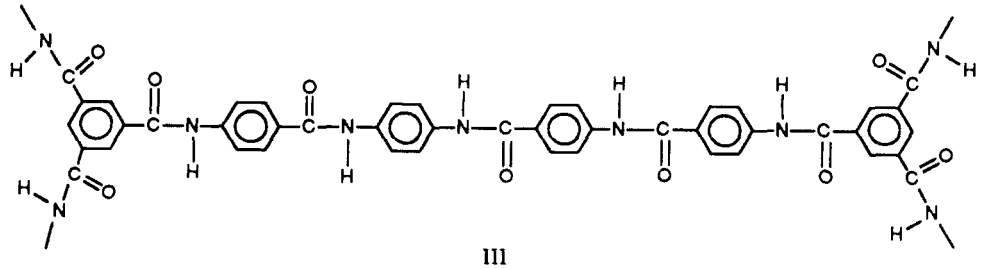

III

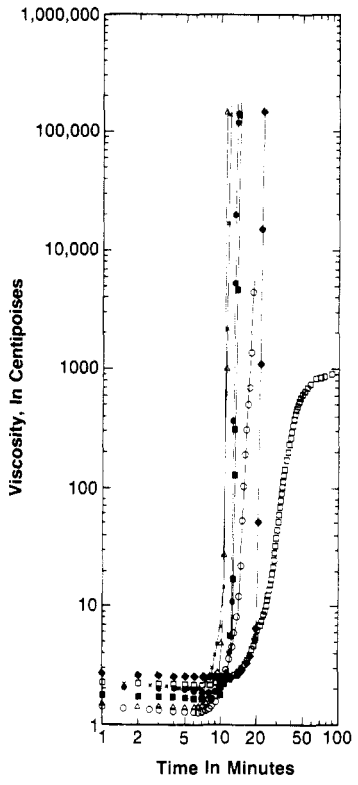

Figure 1. Changes in viscosity with reaction time in the pregel and postgel states of series 37. Systems prepared at 115 °C: rigid and semirigid (●) 37B, (×) 37C, (■) 37D, (○) 37E, (△) 37F: flexible (□) 37G. System polymerized at 103 °C: (◆) 37H. All networks at C_0 = 7.5%.

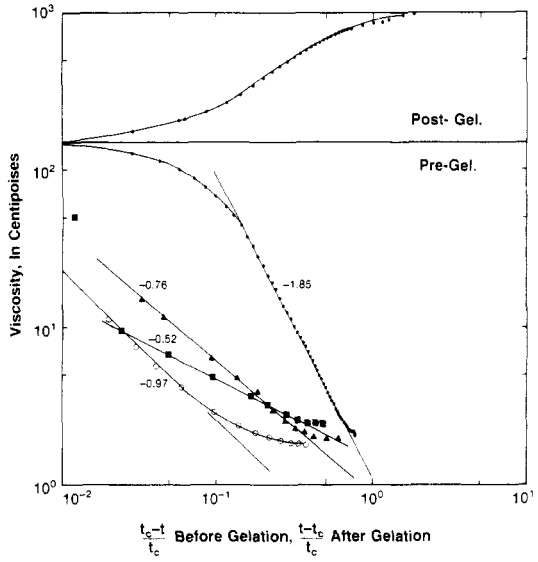

Figure 2. log–log plots of changes in viscosity as a function of reduced time. In the pregel state: (●) 37G, flexible, 115 °C; (⊙) 37B, rigid, 115 °C; (▲) 37C, rigid, 115 °C; (■) 37H, rigid, 103 °C. In the postgel state: only the flexible 37G.

For the purpose of comparison, a few semirigid and flexible systems were prepared, all with the stiff branch-points described above. The semirigid systems, used only for the growth kinetics study, were made by replacing the rigid DABA by bis(*p*-aminobenzoate) trimethylene glycol (BABTMG):

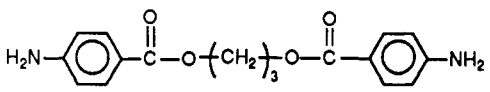

IV

The flexible systems were prepared by the addition of sebacic acid comonomer to the systems containing BABTMG, while maintaining the equality of amine and carboxyl groups.

The changes in viscosity with reaction time of several rigid and semirigid and one flexible member of series 37 are graphically shown in Figure 1. In all instances the gel point was reached when the viscosity was about 200 cP. When the same data were plotted in ref 20 in terms of log reduced viscosity versus reaction time, the data of each rigid or semirigid system fell on one or two straight lines (except for one rigid system polymerized at much lower temperature, which fell on three straight lines). The data points of the flexible system 37G, below the gel point, also fell on two straight lines. log–log plots of the change in viscosity upon approaching the gel point as a function of reduced time, $(t_c - t)/t_c$, indicate that the rigid rod-like systems follow a power law larger than −1 (−0.97 to −0.52), while the viscosity of the flexible system scales as the reduced time to a −1.85 power. Here t_c is the gel time and t is the time when the viscosity was measured. The data are shown in Figure 2, where some postgel results of the flexible system are shown for completeness. A point for the rigid system 37H far away from the extrapolated expectation reflects the fact that at very small reduced time, i.e., very close to the gel point, a large scatter may occur in the data of the rigid systems due to the very steep slope of viscosity versus time in those portions of the curves (see Figure 1).

To study the nature of the growing rigid species in the pregel state, two series were prepared by removing aliquots of the reaction mixture as they increase in viscosity prior to the gel point. After precipitation and careful purification, the various fractions were characterized. The two series, namely, 45X and 59, are fundamentally the same, except that one member of series 59 (59E) was subsequently used for additional synthetic and characterization studies. The monomer composition for both series was 2:1:2/3 molar DABA/nitroterephthalic acid/BTCA. The use of nitroterephthalic acid (NTPA) rendered the systems highly soluble and ensured the amorphicity of the branched polymer, a fact verified by WAXD studies conducted on the bone-dry polymers, on their pastelike concentrated solutions in DMAc/5% LiCl, and on gels of the corresponding "infinite" networks. A typical segment of series 45X and 59 looks like V, and its average length, l_0, is 38.5 Å. Series 45X was prepared in such a monomer concentration that the concentration, C_0, of the resulting polymer network as prepared in the reaction medium will be 3%. The characteristics of the various fractions of the series are shown in Table I.

Table I
Stages in Growth of One-Step Rigid Fractals and Network, l_0 = 38.5 Å, Prepared at C_0 = 3%

code	rctn time, min[a]	polym yield, %	solub in DMAc	intrinsic visc of sol, dL/g[b]	wt av M_w[b]	R_H, Å[b]
45XE	22	10.5	soluble	0.21	7 800	17 ± 2
45XA	27	27	soluble			
45XF	32	35	soluble	0.24	10 700	22.0
45XG	37	70	soluble	0.30	16 700	26.6
45XB	42	79	5.6% gels	1.26	410 000[c]	120
45XH	44	~95	16.0% gels	1.61	700 000[d]	155[d]
45XC	~45	~97	>50% gels[e]			
45XD	55	~98	gelled solid[f]			

[a] Reaction time from the moment TPP was added. [b] Intrinsic viscosity, M_w and R_H of sol fraction alone. [c] The M_w and R_H relate to 67.5% of the sample. The rest is of significantly higher molecular weight in a bimodal distribution obtained by PCS. [d] Estimated from plots of intrinsic viscosity versus M_w and R_H. [e] Gel particles appear in the reaction medium during polymerization. [f] Gelation complete during polymerization.

Series 59 was prepared from the same monomers as series 45X but at a concentration of C_0 = 5%. By the addition of excess 3,4,5-triiodobenzoic acid (TIBA) to the reaction mixture as the viscosity increased and the system was approaching the gel point, we were able to obtain "infinite" networks containing a substantial fraction of blocked segment tips and systems that altogether failed to form a network and solidify. Furthermore, by reacting fraction 59E with itself after it was thoroughly purified of monomers and low-M oligomers, the nature of the rigid branched macromolecules was further elucidated. In the first experiment, 59E was reacted with itself under Yamazaki conditions at C_0 = 10%. A very stiff, isotropic clear gel of a rigid "infinite" network (59F) formed within 2 min from the addition of TPP. In the second experiment, 59E was reacted with a 5-fold excess of TIBA to give 59G. No gelation occurred, even after 30 min reaction time. It is obvious that practically all the accessible amino groups present in the 59E molecules reacted with the TIBA before they had a chance to react with the carbonyl groups of the same or other 59E molecules. In a third experiment, 59E was reacted with a 5-fold excess of 4-iodoaniline to produce 59H. Here, too, no gelation took place. After careful purification, the members of series 59 were characterized by light scattering, iodine analysis and solution properties. The results are listed in Table II. The mechanical properties of the "infinite" networks 59A and 59F will be discussed below together with those of all other gels.

Using light scattering and viscosity data together with the average molecular weight (714) per rigid segment, we employed several relationships previously described by one of us[24] to calculate some characteristic radii and ratios

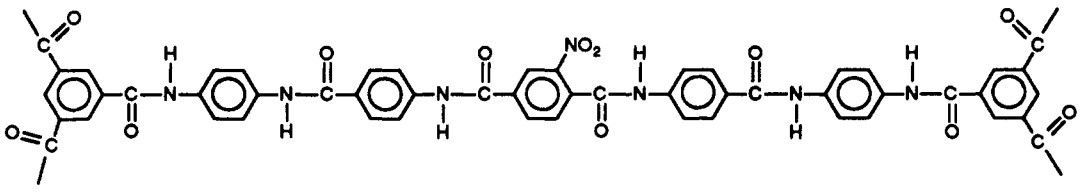

V

of radii to molecular weights. The results, for several fractions of series 45X and for 59E, are tabulated in Table III.

From the M_w and M_w/M_n data obtained by light scattering the PCS, the number-average molecular weight, M_n, of members of the 59 and 45X series in Tables II and III was calculated. From these, the number-average segments, N_n, per branched macromolecule were determined. End-group titrations for carboxyl and primary amine groups gave the equivalent weight per such group, from which one may calculate the number of titratable groups per macromolecule. These numbers are shown in Table IV. In a similar fashion one can calculate from the iodine analysis of 59E, 59G, and 59H the number percent of segments whose tips are decorated by iodine (taking into account the added weight that the extra C, H, N, and O atoms contributed to the segment). The results indicate that amine-terminated segments, decorated with TIBA, amounted to 45.4% of all segments in 59G and carboxyl-terminated segments, decorated with 4-iodoaniline, added up to 39.8% of all segments in 59H. The decorated segments amounted to 85.2% of the total segments in 59E. This is equivalent to 4.6 segments out of the 5.4 segments present in each 59E molecule. The number-average segmental ends, N_{ends}, actually measured is in excellent agreement with the numbers expected by simply modeling each rigid macromolecule with its trifunctional branchpoints and then counting the free segment ends. The calculated number, N_{calc}, is also shown in Table IV. The important results here are the high degree of branching for both 45X and 59 series, the good agreement between the calculated and the measured number of segment ends, and the high accessibility of segment tips to titrant and reactant small molecules, reflecting the free-draining nature of our rigid rodlike one-step highly branched macromolecules.

Plots of intrinsic viscosity $[\eta]$ versus M_w and hydrodynamic radius, R_H, against M_w for series 45X are shown in Figures 3 and 4, respectively. The excellent fit of the four experimental points on both curves gave us confidence in the results and allowed the estimation of M_w and R_H of 45XH from $[\eta]$. The intrinsic viscosity depends on M_w as

$$[\eta] = (5.02 \pm 0.58) \times 10^{-3} M_w^{0.419} \quad (3)$$

and R_H is proportional to M_w as

$$R_H \propto M_w^{0.487} \quad (4)$$

When the M_w/M_n ratios of series 45X are double-logarithmically plotted against M_w in Figure 5, they fall on a straight line defining a power dependence:

$$M_w/M_n \propto M_w^{0.35} \quad (5)$$

The viscosities of three members of the 45X series are plotted in Figure 6 in terms of reduced viscosity (η_{sp}/c) in deciliters per gram versus percent concentration, c. In the dilute solution region the dependence of η_{sp}/c on c is rather small. For sample 45XB, a semidilute interval is observable, with a well-defined linear section of the log–log plot. No such well-behaved interval is observed for the much lower molecular weight 45XG. Beyond 5% concentration, 45XB reaches its concentrated solution regime with a higher linear dependence of η_{sp}/c on c. We have insufficient data on 45XG in the concentrated regime to estimate the power dependence of its reduced viscosity on concentration. The dilute solution results of 45XB indicate that viscosities obtained by the glass

Table II
Characteristics of Pregel and Postgel One-Step Rigid System with l_0 = 38.5 Å

code	C_0, %	iodine, wt %	% gel	intrinsic visc of sol, dL/g	M_w[a]	M_w/M_n[a]	M_n	R_H,[a] Å
59C	5	ND[b]	none	<0.24	3 300	1.8	1850	10.4
59E	5	none	none	0.26	9 600	2.5	3850	18.1
59G	3	21.35	none	0.27	16 400	2.8	5850	21.6
59H	3	6.23	none	0.27	12 200[c]	2.8[c]	4350[c]	ND
59B	5	12.69	14.1	1.38	780 000	5.0	156000	124
59D	5	none	52.9	1.61	ND	ND	ND	ND
59A	5	7.60	>90					
59F[d]	10	none	>98					

[a] By light scattering and PCS. [b] Not determined. [c] From iodine analysis and measured values of 59E. [d] Prepared from purified 59E.

viscometer (at 25 °C) and the Nametre viscometer (at 23 °C) are reasonably close to one another. We conclude that for sample 45XB we observe three well-defined regions of dependence of η_{sp}/c on c:

$$\eta_{sp}/c \propto c^{0.20}; \quad c < 1.2\% \quad (6a)$$

$$\eta_{sp}/c \propto c^{0.79}; \quad 1.2\% < c < 5\% \quad (6b)$$

$$\eta_{sp}/c \propto c^{2.04}; \quad 5\% < c < 26\% \quad (6c)$$

We have insufficient data to correlate the different power laws above with expected fractal behavior in different concentration regimes.

The intensity, $I(q)$, of X-rays scattered as a function of the scattering vector, q, was measured on several members of the 45X series in a bone-dry state and as a usually clear paste consisting of 1 part by weight polymer and 2 parts DMAc/5% LiCl. A typical plot of intensity versus 2θ, demonstrating the difference in scattering intensity between a polymeric pastelike solution and the pure DMAc/5% LiCl solvent mixture, is shown in Figure 7. The background-corrected intensities were then plotted as log $I(q)$ against log q, as is shown in the two panels of Figure 8. Within the range of accessible q the data points fall on rather linear curves with slopes as listed in Table V. The results of the 1:2 paste are especially instructive since they were obtained from the branched macromolecules swollen with solvent, bringing them closer to the shape and behavior expected of them in dilute solution. The bone-dry ones may have collapsed and lost some features of their original geometry. It is well accepted in the literature[22,23,25-28] that in this range of q, a dependence of $I(q)$ on q to a power of less than 4, especially a noninteger dependence, is indicative of a fractal nature of the scattering sample.

The critical concentration for gelation, C^*_0, of the one-step rigid rodlike networks was found to be dependent on the length, l_0, of the segments between branchpoints. In this study systems were prepared with trifunctional stiff branchpoints and segments as short as 6.5 Å and as long as 65 Å, the former from equimolar amounts of 5-aminoisophthalic acid and 3,5-diaminobenzoic acid, and the latter from 2:1:2/3 DABA/4,4′-dibenzoic acid terephthalamide/TCPBT. The 4,4′-dibenzoic acid terephthalamide was prepared by a Schotten-Baumann type reaction from *p*-aminobenzoic acid and terephthaloyl dichloride. Networks with intermediate segment length were polymerized in a similar fashion from combinations of the monomers used throughout this work. Each polymer was prepared in several concentrations, C_0, until a concentration interval was reached where the formed gel did not encompass the whole volume of the reaction

Table III
Dilute Solution Characteristics of Pregel One-Step Highly Branched Rigid Macromolecules[a]

code	intrinsic visc	M_w	N_w	M_z/M_w	R_H, Å	R_{Gg}, Å	R_{Gvisc}, Å	R_{Gfd}, Å	R_{Gnd}, Å	$R_H/M_w^{1/2}$	$R_{Gvisc}/M_w^{1/2}$
45XE	0.21	7 800	11	1.7	17 ± 2	52	34.6	22.7 ± 1.3	12.5 ± 0.5	0.193 ± 0.022	0.392
45XF	0.24	10 700	15	1.5	22.0	61	40.2	24.8	13.65	0.213	0.389
45XG	0.30	16 700	23.4	1.6	26.6	76	50.2	31.6	17.4	0.206	0.388
45XB	1.26	410 000	574	1.8	120	377	235.8	150.9	83.1	0.187	0.368
45XH	1.61	700 000[b]			155[b]						
59E	0.26	9 600	13.4	1.6	18.1	57.5	39.9	27.0	14.9	0.185	0.407

[a] Intrinsic viscosity in dL/g. M_z/M_w from diffusion coefficient distributions measured by PCS. R_{Gg} = Gaussian radius of gyration; R_{Gvisc} = viscosity-derived radius of gyration; R_{Gfd} = freely draining radius of gyration; R_{Gnd} = nondraining radius of gyration; R_H = hydrodynamic radius. [b] Extrapolated from log–log plots.

Table IV
Number of End Groups per Macromolecule of Members of the 45X and 59 Series

code	M_w	M_w/M_n	M_n	N_w	N_n	N_{ends}[a]	N_{calc}
45XE	7 800	(2.0)	3900	11	5.5	4.1	4–5
45XF	10 700	2.2	4860	15	6.8	5.8	6
45XG	16 700	2.7	6200	23.4	8.7	6.9	7
45XB	410 000	8.6	47650	574	67	37	35
59E	9 600	2.5	3850	13.4	5.4	4.6	4–5

[a] 45X by end-group titration and 59E by iodination of segment tips in 59G and 59H.

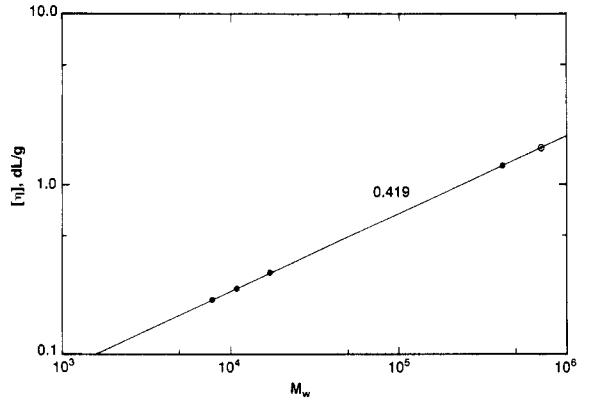

Figure 3. log–log plot of intrinsic viscosity versus M_w of series 45X. All in DMAc/5% LiCl solution; (⊙) extrapolated.

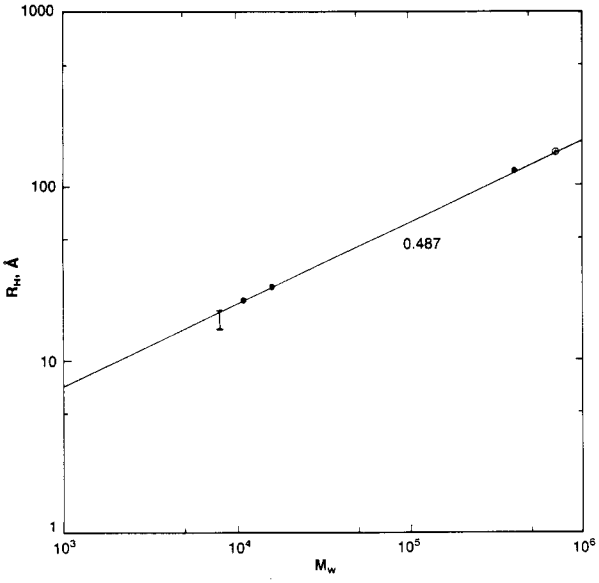

Figure 4. Hydrodynamic radius versus M_w of series 45X. In DMAc/5% LiCl solution; (⊙) extrapolated.

mixture. This point is taken by us to be C^*_0: at $C_0 > C^*_0$ the whole volume was gelled and at $C_0 < C^*_0$ a smaller and smaller fraction of the total sample was gel. To these data we added previous data, especially on systems with

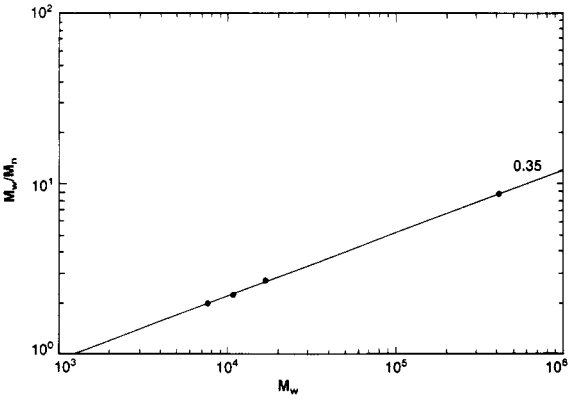

Figure 5. M_w/M_n ratio as a function of M_w of series 45X.

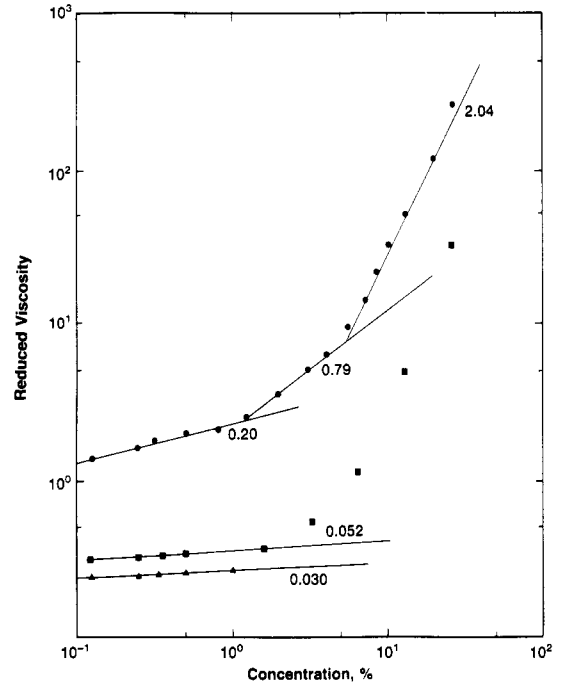

Figure 6. Reduced viscosity as a function of concentration for members of the 45X series in the pregel state: 45XB (●) in a Nametre direct readout viscometer at 23 °C; (■) 45XG in a Nametre viscometer at 23 °C; (▲) 45XF in a glass viscometer at 25 °C.

very long segments, taken from Aharoni and Wertz.[19] All the results are plotted in Figure 9. The C^*_0 versus l_0 curve obviously separates into two branches. The branch with $l_0 > 65$ Å is associated with different behavior of the gel right above C^*_0 than the branch for $l_0 \leq 65$ Å. The gels of the long segments were extremely soft and could not retain the shape of the reaction vessel once removed from it. Conversely, the gels of the $l_0 \leq 65$ Å segments maintained their shape, being relatively stiff at l_0 close to 65 Å with considerable increase in brittleness as l_0 became shorter. Based on the above, we believe

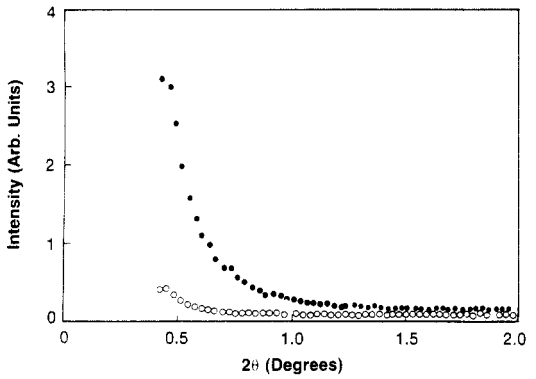

Figure 7. Typical absorption-corrected SAXS curves for a 45XB pastelike 1:2 solution in DMAc/5% LiCl (●) and DMAc/5% LiCl solvent mixture (○). While the data were collected at 2θ intervals of 0.016°, for clarity data obtained by averaging over every 0.03° intervals are shown in the figure.

that the softness and deformability under gravity of the $l_0 > 65$ Å gels is due to the inability of the very long segments and resultant loosely connected network to support the weight of the occluded solvent. In the case of $l_0 \leq 65$ Å, a different situation exists. Here, the decreasing distances between branchpoints of the growing particles simply deplete the reaction mixture of monomeric species and prevent the formation of "infinite" networks. This depletion is compensated by increasing the total monomer concentration in the reaction mixture until a point is reached where an "infinite" network is finally formed. Conversely, as the segment length increases from 6.5 to 65 Å, the growing network can accommodate within it a larger and larger fraction of the reaction solvent, allowing C^*_0 to fall toward $l_0 \cong 65$ Å. This picture is also consistent with the increasing time periods with decreasing l_0 required for the gel point to be reached (over 4 h for $l_0 = 6.5$ Å).

Well-dried powders of the one-step rigid fractions 45XF and 45XB were sputtered with gold and then observed at 60000× magnification in a scanning electron microscope (SEM). Their nodular structure, in Figure 10A,B, is immediately evident. The appearance of 45XB is especially reminiscent of the morphologies of fractal growth of several diverse systems reported in the literature.[29-33] The size of the smallest observed nodules is in fair agreement with the size of the rigid fractals deduced from their R_H values in Table I. A very fine mottled texture, much smaller than 100 Å in size, which can be seen in the original micrographs, is ascribed to the sputtered gold. The materials for Figure 10C,D were obtained from the gelled networks of the flexible polymers 51B and 51C (to be described below) by passing them through a blender and then extracting the solvent, drying, and preparing for SEM observation as has been described in the Experimental Section. Their surfaces are smoother than those of the rigid networks and instead of the obvious nodular texture of the rigid networks, the dried flexible networks exhibit surfaces reminiscent of the appearance of a mammalian cerebral cortex.[29] The texture of the two-step network 51B is finer than the corresponding texture of 51C, indicating a measure of dissimilarity between the two flexible networks. However, because of the flexibility of the polymers, it is most unlikely that there will be evident a direct correlation between the size and shape of the dried-up, collapsed aggregates and their solvent-filled analogues in solution.

(b) Gelled Networks. Rigid one-step gelled networks were prepared by the Yamazaki procedure as described above. The networks were prepared neat and with filler macromolecules at concentrations C_0 as shown in Table VI. The modulus of the gelled networks was measured at ambient temperature on the as-prepared gels (at C_0) and on gels that were allowed to equilibrate with DMAc (at C). The preparation and characteristics of the filler macromolecules, including three high-M polymers of high and low rigidity and a monodisperse rigid oligomer, are described in section c. With the exception of several rigid one-step systems used for the growth kinetics studies, all rigid one-step gelled networks whose moduli were measured in this study were chemically identical, with the same average segment length, $l_0 = 38.5$ Å, between stiff trifunctional branchpoints as described in structure V and with respect to the reaction conditions after gelation occurred. These networks fall into three series: (a) gel 59A in which some segment tips were decorated with iodine and gels 59F and 59J made from the carefully purified 59E fractals described above; (b) members of series 45X that were allowed to further react and

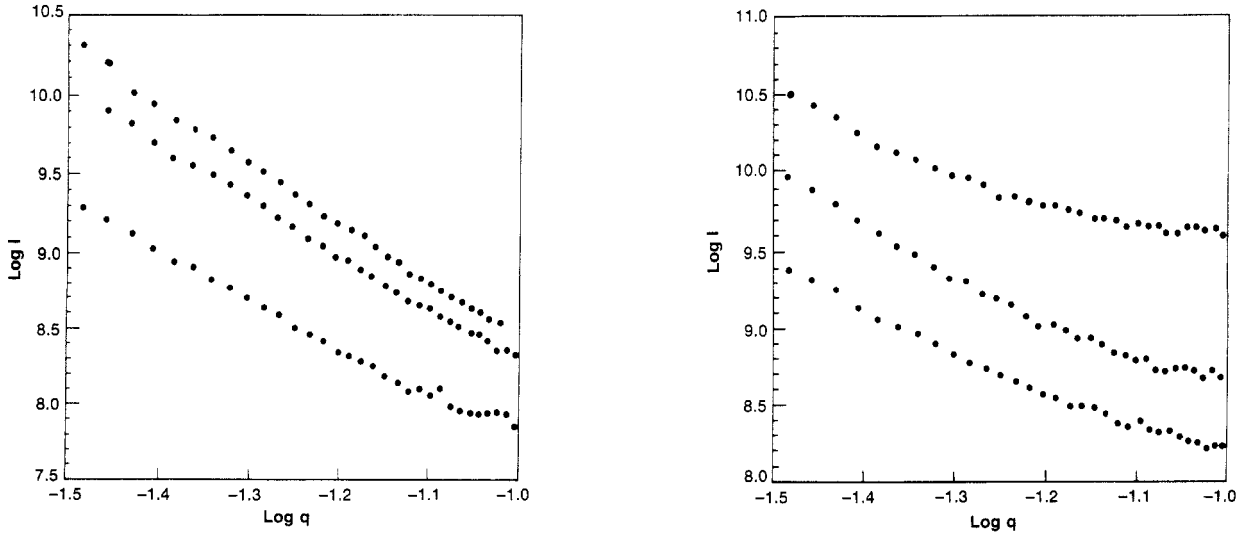

Figure 8. Intensities of SAXS versus q of three representative pregel (45XE and 45XB) and postgel (45XD) rigid rodlike, trifunctional, highly branched systems, plotted on the log–log scale. For clarity, each data point set is displaced vertically by 0.5 log I unit. The number of points along each curve is reduced for clarity in the same manner as in Figure 7. Left panel: Bone-dry 45XE (top), 45XB (middle), 45XD (bottom). Right panel: Solvent-swollen samples (1:2 polymer/solvent); 45XE (top) (scattering exponent for this sample was obtained from only the small-q portion of the curve), 45XB (middle), 45XD (bottom).

Table V
Scattering Exponents and D_s Values for Several Members of the 45X Series[a]

		dry samples		solvent-swollen samples	
code	form	scattering exponents	D_s	scattering exponents	D_s
45XE	pregel	3.75	2.25	3.5	2.5
45XF	pregel	3.5	2.5		
45XG	pregel	4.0	2.0	3.3	2.7
45XB	pregel	3.9	2.1	3.35	2.65
45XD	network	3.3	2.7	3.0	3.0

[a] Values rounded within ±0.05.

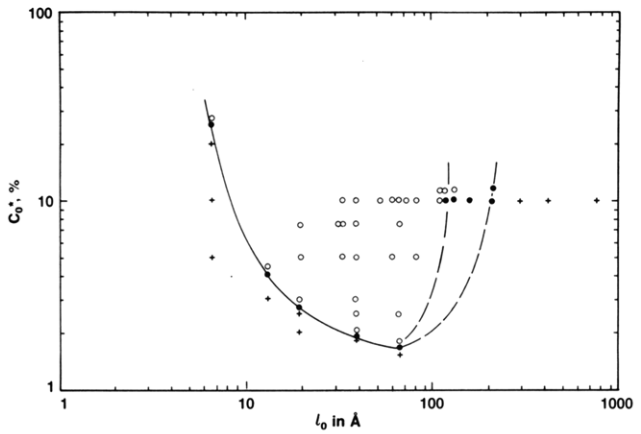

Figure 9. log–log plot of the critical concentration for gelation, C^*_0, as a function of segment length, l_0: (○) system gelled; (+) system did not gel; (●) system at the gel point, mostly gelled but some sol regions. Often the formed gel in this concentration interval would not maintain its shape after being removed from the reaction vessel.

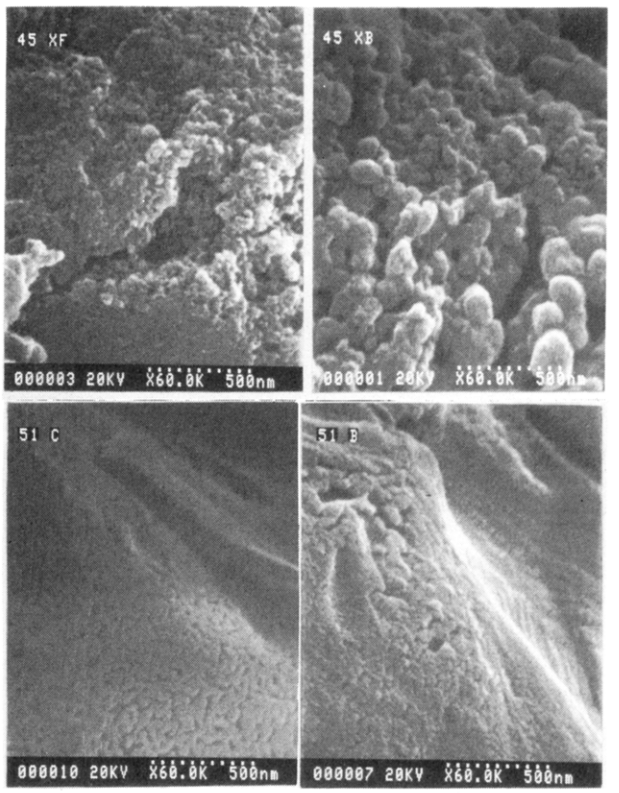

Figure 10. (A) SEM photograph of the surface of one-step rigid polymer 45XF powder. Note nodular structures down to about 250 Å. (B) Same for one-step rigid polymer 45XB. Note several size scales of nodules, the smallest appear to be about 400–500 Å in diameter. (C) Same for one-step flexible polymer 51C. Surface appears as the cerebral cortex of upper mammalian animals with promontories about 1000 Å in width. (D) Same for two-step flexible polymer 51B. Here the surface is more fine grained, with features only about 300 Å in size. The dotted line at the bottom right of each micrograph is 5000 Å long.

form "infinite" networks; (c) members of series 45 (45B2 through 45T and 48C) in Table VI.

The gelled networks of series 59, especially 59F and 59J, which were prepared from the fractals 59E in the complete absence of monomers and low-M oligomers, are remarkable and merit special mention. Their characteristics are listed in Table VII together with those of chemically identical one-step rigid gelled networks previously prepared from monomers in the conventional manner.

Importantly, series 59 shows that the fractals 59E can easily react under Yamazaki conditions with one another to form an "infinite" network in the absence of any monomers or low-M oligomers. The formation of an "infinite" network occurs at the same concentrations as in the presence of monomeric species. In fact, the gelation is much faster than the gelation in the regular one-step polymerizations under similar concentrations. The moduli of the as-prepared gelled networks are higher than or similar to those of the comparable regular networks. During equilibration in DMAc the gels swell substantially less than the comparable regular one-step gels and the modulus of the equilibrated gels is, hence, higher than that of the regular gels. Sample 59A shows that if the reaction is allowed to proceed far enough, an infinite network can develop from partly blocked fractals. It should be noted that the blocking/iodination reagent used here blocks only amine-terminated segments. When the addition of the iodination reagent is done a little earlier in the reaction, compare 59B in Table II with 59A, the formation of an "infinite" network is prevented and some gel particles remain in the reaction mixture together with very high-M highly branched soluble polymeric fractals.

A series of flexible one-step gelled networks listed in Table VIII was prepared in a similar fashion. All but one (51C) of the tabulated flexible systems (series 45E2 through 45R) used a dimer acid as a flexibilizing monomer. In this case the average segment length between tri-

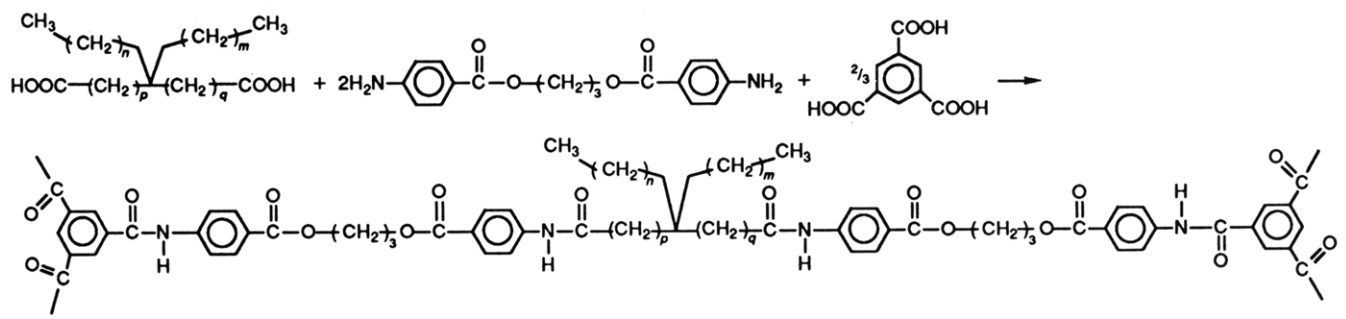

VI

Table VI
Modulus of One-Step Rigid Rodlike Network Gels, l_0 = 38.5 Å[a]

code	description	C_0, %	modulus at $c = C_0$, dyn/cm²	% wt loss during DMAc equilibrat	equilibrated $c = C$, %	modulus at $c = C$, dyn/cm²
45B2	neat network	10.0	3.06×10^6	methanol sol very little	7.4	2.29×10^6
45C2	neat network	7.5	2.45×10^6	methanol sol very little	5.3	1.88×10^6
45D2	network + rodlike	7.5 + 2.5	1.68×10^6	15.9% of total	5.06/6.75	1.41×10^6
48C	network + oligomer	7.5 + 2.5	2.41×10^6	6.6% of total	4.94/6.59	1.82×10^6
45J2	network + X's	7.5 + 2.5	1.95×10^6	10.7% of total	4.91/6.55	1.73×10^6
45V	network + flexible	7.5 + 2.5	2.06×10^6	0.17% of total	4.96/6.62	1.60×10^6
45P	neat network	5.0	2.28×10^6	3.1%	3.36	1.53×10^6
45M	network + rodlike	5.0 + 5.0	1.51×10^6	10.9% of total	3.08/6.17	1.07×10^6
45K	network + X's	5.0 + 5.0	0.71×10^6	19.9% of total	2.83/5.65	0.68×10^6
45T	network + flexible	5.0 + 5.0	1.24×10^6	0.28% of total	3.39/6.77	0.94×10^6
59A	neat iodinated network	5.0	0.66×10^6	not measd	4.32	0.595×10^6
59F	neat network from fractals	10.0	3.80×10^6	none detected	9.20	3.54×10^6
59J	neat network from fractals	5.0	2.19×10^6	none detected	4.12	2.09×10^6

[a] All measurements were performed at 23 °C. In systems with fillers, the majority of the extracted material was filler material. In the DMAc-equilibrated systems with fillers, the larger number was experimentally determined while the smaller number was calculated on the basis of the charge ratio in the C_0 column.

Table VII
Chemically Identical One-Step Rigid Gelled Networks

code	as-prepared $c = C_0$, %	how & from what made	modulus, dyn/cm²	equilibrated in DMAc, $c = C$, %	modulus, dyn/cm²
45B2	10.0	monomers, regular	3.06×10^6	7.4	2.29×10^6
59F	10.0	fractals 59E	3.80×10^6	9.20	3.54×10^6
45P	5.0	monomers, regular	2.28×10^6	3.36	1.53×10^6
59J	5.0	fractals 59E	2.19×10^6	4.12	2.09×10^6
59A	5.0	monomers, partly blocked, regular	0.66×10^6	4.32	0.595×10^6

Table VIII
Modulus of One-Step Flexible Network Gels, l_0 = 58 Å[a]

code	description	C_0, %	modulus at $c = C_0$, dyn/cm²	% wt loss during DMAc equilib	equilibrated $c = C$, %	modulus at $c = C$, dyn/cm²
45E2	neat network	10.0	1.40×10^6	2.5%	5.46	1.25×10^6
45G2	neat network	7.5	1.27×10^6	2.27%	3.83	0.95×10^6
45F2	network + rodlike	7.5 + 2.5	0.815×10^6	8.19% of total	2.82/3.76	0.49×10^6
45H2	network + X's	7.5 + 2.5	0.332×10^6	10.09% of total	2.61/3.48	0.24×10^6
45S	network + flexible	7.5 + 2.5	0.348×10^6	0.38% of total	3.61/4.81	0.24×10^6
45Q	neat network	5.0	1.03×10^6	methanol sol very little	3.01	0.73×10^6
45N	network + rodlike	5.0 + 5.0	0.0192×10^6	25.8% of total gels	2.62/5.24	0.014×10^6
45L	network + X's	5.0 + 5.0	did not gel	100% soluble		
45R	network + flexible	5.0 + 5.0	0.199×10^6	0.69% of total	2.17/4.33	0.096×10^6
51C	neat network	10.0	0.94×10^6	3.2%	4.39	0.48×10^6

[a] Explanations as in footnote for Table VI. Network 51C has l_0 = 52 Å.

functional stiff branchpoints is l_0 = 58 Å. The other flexible one-step network (51C) was prepared by the same procedure from 4:2:3 M dodecanedioic acid/3,5-diaminobenzoic acid/BABTMG, producing the idealized structure VII having an average segment length of l_0 = 52 Å.

A two-step analogue (51B) of the above was prepared by first reacting dodecanedioyl dichloride with 3,5-diaminobenzoic acid and BABTMG under Schotten-Baumann-type conditions to form a high-M linear polymer, VIII. Its intrinsic viscosity was 0.71 dL/g and its M_w is estimated[34] at around 50 000. In the second step,

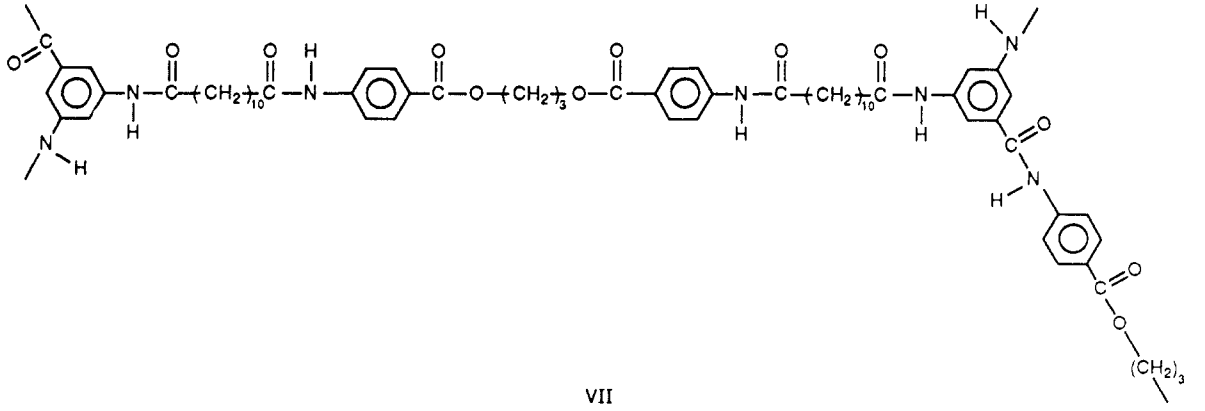

VII

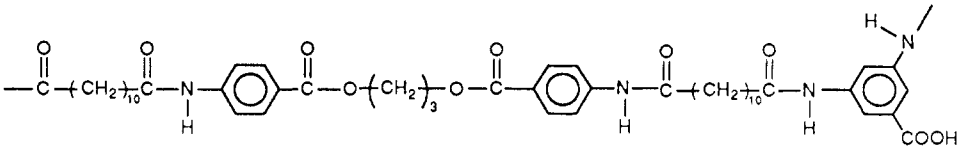

VIII

each mole of repeat units of the linear polymer was reacted under Yamazaki conditions with 0.5 mol of Polacure to form a gelled network. Its characteristics are given in Table IX.

The flexible gelled networks 51B and 51C were prepared under identical conditions: Yamazaki procedure with the same amounts of DMAc/5% LiCl, pyridine, and TPP in both instances, at identical temperature (108 °C) and for identical residence time (3 h) after gelation. The dramatic difference in modulus between the two systems indicates that the two-step network is fundamentally different from the one-step network, even though they are chemically identical and were cross-linked under identical conditions. Similar differences are present also between the higher modulus two-step rigid rodlike networks in Table IX and their one-step analogues in Table VI. Interestingly, one-step and two-step networks prepared at a similar concentration C_0 appear to swell about the same amount during equilibration in DMAc. It may be that the swelling reflects gross average cross-link density and fails to recognize local variability.

For the rigid two-step gelled networks in Table IX, a linear rigid chain was first prepared by a Schotten-Baumann-type reaction (IX). The intrinsic viscosity of this chain was measured to be $[\eta] = 0.35$ dL/g, resulting in an estimated[35] $M_w = 10\,000$. In the second step these chains were reacted under Yamazaki conditions with the appropriate amounts of DABA, in the presence or absence of the rigid rodlike filler macromolecules, to produce a highly cross-linked gelled rigid network, X. In this case the network is characterized by two segmental lengths present in about equal numbers, an average $l_0 = 33.9$Å and a fixed $l_0 = 19.5$Å.

The moduli of the as-prepared systems, at $c = C_0$, and of the DMAc-equilibrated systems, at $c = C$, are listed in Tables VI, VIII, and IX, together with C_0 and C, and the nature and weight percent of material extracted out of the gelled networks during DMAc equilibration.

It is important to emphasize that all but one (51C) of the gelled networks listed in Tables VI–VIII were transparent, with no optical blemishes and, due to their color, appeared as tinted glass. The clarity of the gels was retained and on occasion improved (e.g., 51C, which changed from transluscent to perfectly transparent) after equilibration in DMAc. The high optical quality of the network gels indicates that no microsyneresis on a scale greater than about 1000 Å in the networks themselves took place and that the filler macromolecules do not phase separate from the forming network gel to an extent that haze or transluscence become detectable. The chemical similarity of the fillers and networks obviously enhances their mutual compatibility.

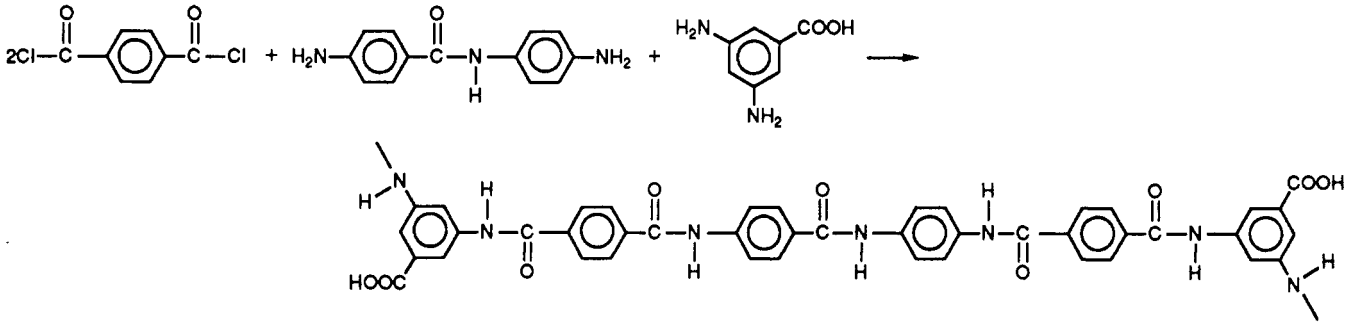

IX

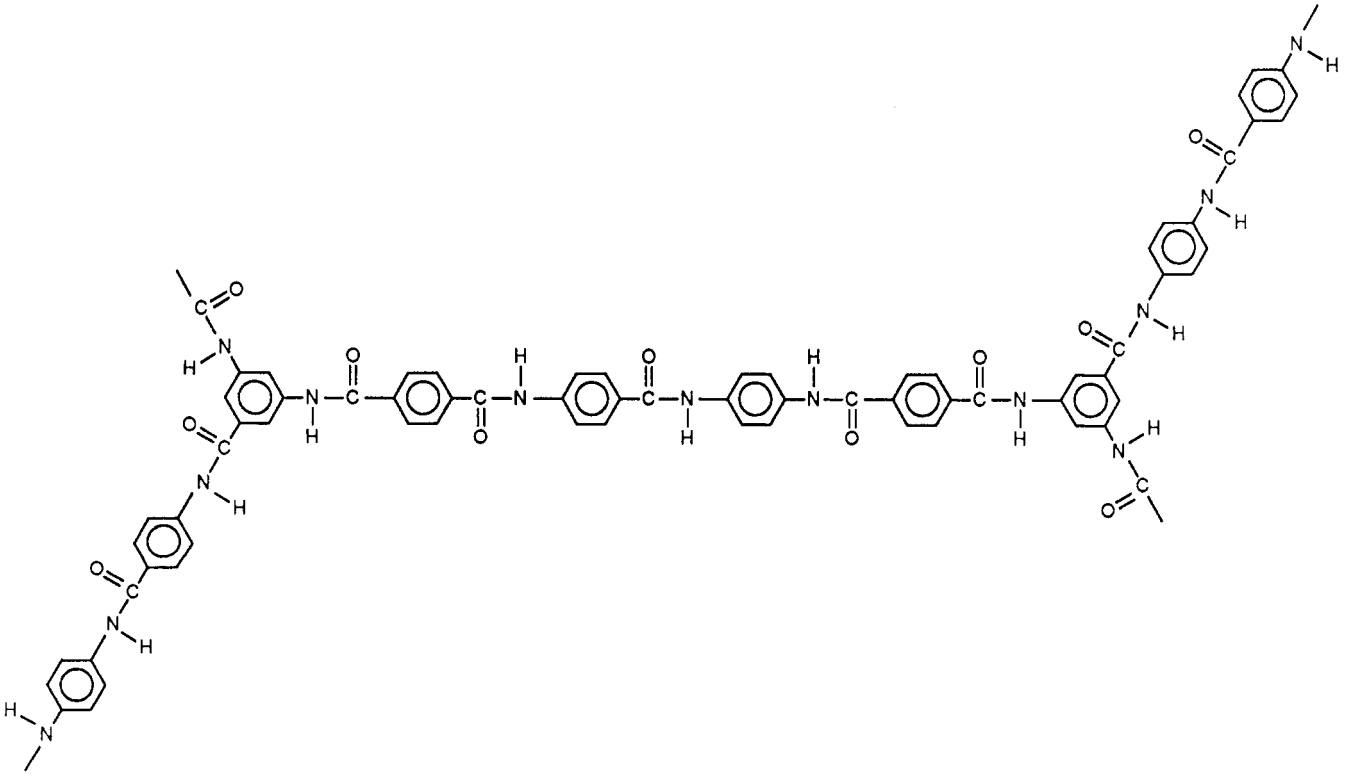

X

Table IX
Modulus of Two-Step Network Gels[a]

code	description	C_0, %	modulus at $c = C_0$, dyn/cm²	% wt loss during DMAc equilib	equilibrated $c = C$, %	modulus at $c = C$, dyn/cm²
49A1	neat rigid network	10.0	4.48×10^6	methanol sol very little	7.04	2.58×10^6
49A2	neat rigid network	7.5	2.91×10^6	methanol sol very little	5.46	2.28×10^6
49A3	rigid network + rodlike filler	7.5 + 2.5	3.28×10^6	0.31% of total	5.03/6.70	2.87×10^6
51B	neat flexible network	10.0	1.78×10^6	0.2%	5.72	0.95×10^6

[a] The rigid systems has $l_0 = 33.9/19.5$ Å and the flexible one has $l_0 = 52$ Å. All other explanations as in Table VI.

Wide-angle X-ray patterns were obtained from several rigid and flexible, as-prepared and DMAc-equilibrated gels. They exhibited only amorphous halos, indicating that no detectable crystallinity was present in them. To be detectable, crystallites of 35 Å or more must be present in volume fractions of 0.01 and over. This is not surprising in light of the low network concentration in the gels and the low degree of crystallinity expected, at best, in gels where the segments are relatively short and randomly distributed in space. Furthermore, it was found that all rigid rodlike networks containing the nitroterephthalic residue were amorphous in both swollen and fully dried states.

Infrared spectra obtained as described above indicated that the intensity of the 3400-cm^{-1} band is very small in the case of the linear rigid filler polyamide and that its relative intensity increases substantially in the chemically comparable rigid network. This indicates that the shorter the segment between branchpoints the poorer the chains can pack and the smaller the fraction of segment–segment H bonds. Additional IR studies[36] on rigid networks with varying segment length led to the same conclusion.

When the solvent in the one-step rigid network gels was removed and the networks were fully dried, many of them were very ramified and others appeared under the microscope to be highly corrugated and craggy. We have noted that the corresponding gels showed a propensity to crack when prepared at concentrations right above C^*_0 and during relatively rapid changes in temperature for all $C_0 > C^*_0$. We believe that both these observations suggest an internal inhomogeneity of the gels, even though they appear optically to be blemishless and the gels behaved as uniform isotropic gels in all tests. Dried small particles collected from one-step preparations too dilute to form self-supporting "infinite" network gels appeared under the optical microscope to be highly ramified at all observable length scales. This is in agreement with the SEM observations typified by Figure 10A,B.

To quantify the porosity of bone-dry rigid rodlike networks, we elected to study a representative one, namely, 45XC. The material was prepared by chopping the gelled network in a blender, followed by careful sol extraction, washing in methanol, and, finally, thorough drying at 120 °C under high vacuum. It was measured by three techniques sensitive to smaller and smaller pores. Conventional pycnometry in CCl_4/hexanes resulted in density, d, of 0.962 g/cm³. Mercury porosimetry yielded $d = 1.277$ g/cm³. This technique is capable of detecting pores as small as 36 Å under the pressures used in this study. We elected to count all pores smaller than 10 000 Å. This pore-size interval, 36–10 000 Å, gave 9.9% pore volume. The third technique is helium pycnometry, which is sensitive to pores smaller than 36 Å in diameter. It gave a density of $d = 1.411$ g/cm³ and 8.6% pore volume. We find, hence, that for pores smaller than 10 000 Å, the total pore volume is 18.5%. The density of the dry 45XC particles as measured by mercury porosimetry prior to the aplication of pressure was 0.898 g/cm³, a reasonable value considering that the surface energy of mercury is higher than that of the organic mixture employed in the conventional pycnometry. From the added weight of the 45XC particles, an organic liquid accessible void fraction of 46% measured. A plot of density versus percent pore volume for the three techniques ($d = 1.411$ g/cm³/8.6%; $d = 1.277$ g/cm³/18.5%; $d = 0.962$ g/cm³/46%) defines a straight line (not shown here), which extrapolates to $d = 1.51$ g/cm³ at zero pore volume. Such high density is very close to that of 100% crystalline un-crosslinked oligomeric linear aromatic polyamides, whose average density, $d = 1.48$ g/cm³, was measured by conventional pycnometry[35] and is in close proximity to the crystallographically expected density of 1.53 g/cm³.[35] Recalling that WAXD showed sample 45XC to be fully amorphous, we reach the conclusion that helium does penetrate into the amorphous phase of the highly branched 45XC material and may not penetrate the crystalline phase of the linear analogue. The density difference of 1.53 − 1.41 = 0.12 g/cm³ reflects the dilatation of the polymeric material upon going from the fully crystalline to the fully amorphous phase, plus the contribution of pores smaller than 36 Å in diameter. Recalling that the average segment length in 45XC is 38.5 Å, such pore sizes appear to be smaller than the length of a single rigid segment.

(c) Filler Macromolecules. Four filler substances were prepared, three of them polymeric and one a monodisperse oligomer with four aromatic rings per molecule. A linear rigid macromolecule was prepared from DABA and nitroterephthalic acid (NTPA) (XI). The second macromolecular filler has an idealized X shape with each arm averaging eight aromatic rings in length. It was prepared in two steps. In the first, a Schotten-Baumann-type reaction was used to prepare the rigid tetrafunctional core XII.

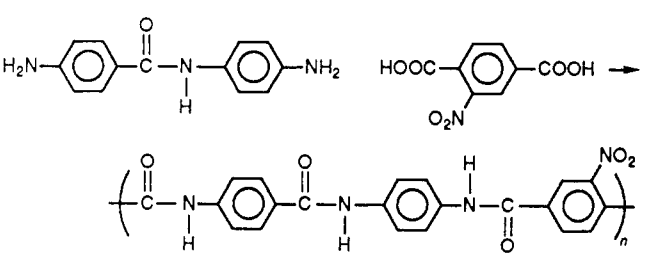

XI

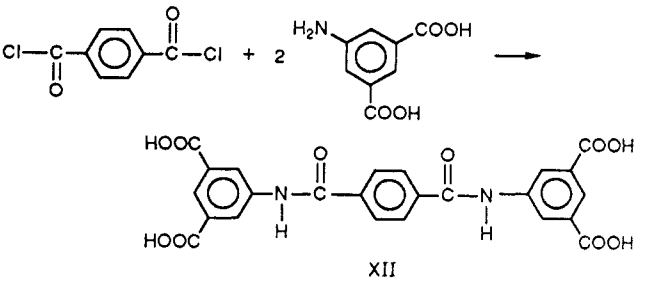

XII

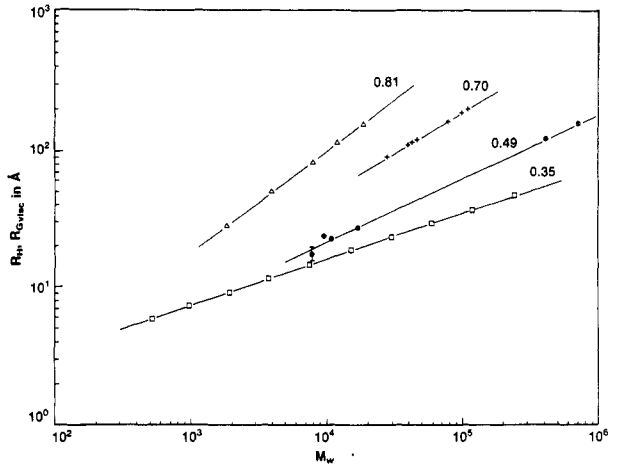

Figure 11. log–log plot of radii of polyamides of differing rigidity and branching as a function of M_w. Power laws marked near each straight line. (△) Rigid rodlike linear poly(*p*-benzanilide terephthalamide) (PBT), R_{Gvisc}. (+) Poly(ϵ-caprolactam), R_{Gvisc}. (●) 45X series and 59E branched rigid fractals, R_H. (□) Boc-poly(α,ϵ-L-lysine), flexible, branched, R_H and R_{Gvisc}.

After workup and purification, this product was reacted in a Yamazaki procedure with a 32-fold molar amount of *p*-aminobenzoic acid. The *p*-aminobenzoic acid was added to the reaction mixture in very small increments over several hours, to maximize the chances of creating X's and to minimize the formation of linear poly(*p*-benzamide). The idealized shape of the product is XIII. A

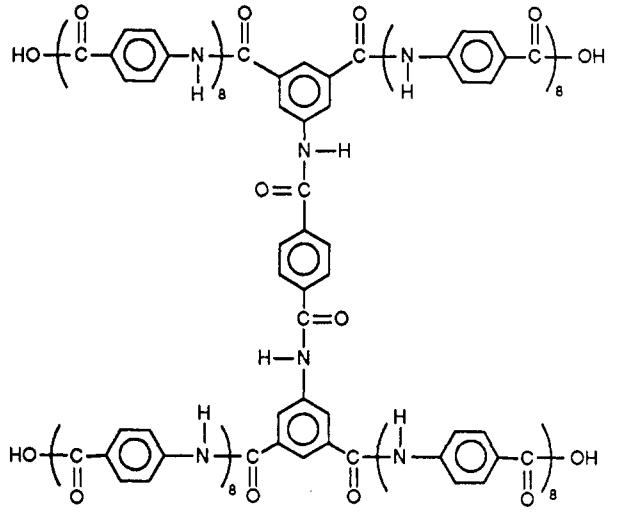

XIII

flexible linear macromolecule was prepared from BABTMG and dimer acid (XIV).

The short monodisperse oligomer was prepared by Yamazaki procedure from *m*-nitrobenzoic acid and DABA (XV). This material melts and decomposes at 350 °C.

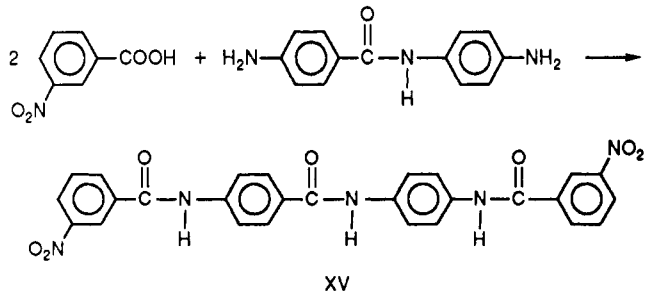

XV

Intrinsic viscosity and light scattering measurements for the rodlike filler macromolecules were $[\eta] = 0.83$ dL/g and $M_w = 12\,700$. These values are in fair agreement with expectation.[35] The intrinsic viscosity of the flexible filler macromolecule, $[\eta] = 0.40$ dL/g, results in an estimated[34] molecular weight of $M_w \cong 20\,000$. For the X-shaped filler macromolecules, values of $[\eta] = 0.224$ dL/g and $M_w = 10\,000$ were measured. Assuming strict linearity, the molecular weight calculated from viscosity[35] is supposed to be only 2200. The discrepancy between the actual and calculated M_w clearly indicates that the X-shaped macromolecules are branched and not linear.

The molecular weight of the rodlike macromolecules corresponds to a weight-average degree of polymerization (DP) of 106. Allowing 6.5 Å per aromatic ring with a para-amide group, this results in a weight-average length of 690 Å. Our past experience teaches us that for these polyamides, prepared under the Yamazaki conditions, $M_w/M_n \cong 1.75 \pm 0.1$. This leads to a number-average estimate of $L = 390$ Å, L being the end-to-end length of the macromolecule. Branched macromolecules produce larger polydispersity, and for the size calculation of the rigid X's, we adopt $M_w/M_n = 2$ as a good estimate. From the measured M_w, we calculate a number-average DP of 38 in addition to the tetrafunctional nucleus. This is reasonably close to the DP = 32 expected from the monomer charge. The difference may reflect a deviation from $M_w/M_n = 2$. The value of DP = 38 results in $L \cong 140$ Å. The length of the monodisperse oligomer is about 24 Å. Based on molecular weight per repeat unit of 843, one obtains for the flexible filler macromolecules a weight-average DP of about 24, and an estimated number-average DP of 12. The calculated chain length per repeat unit is about 46 Å, resulting in number-average $L = 550$ Å. The flexible filler macromolecules are supposed to be randomly coiled. Because of the high backbone flexibility, a freely jointed Gaussian chain behavior is expected:[24]

$$R_{Gg} = l(N/6)^{1/2} \tag{7}$$

Here, R_{Gg} is the Gaussian radius of gyration, l is the length of a Kuhn segment, and N is the number of such segments per chain. In our case, eq 7 leads to $R_{Gg} = 65$ Å.

Plots of reduced viscosity against concentration (not

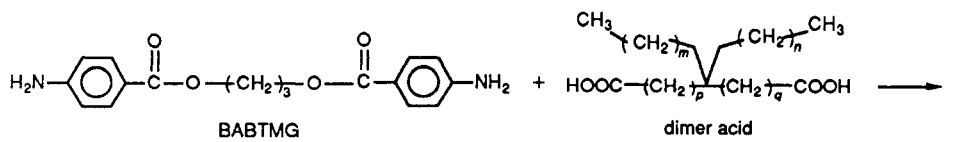

BABTMG dimer acid

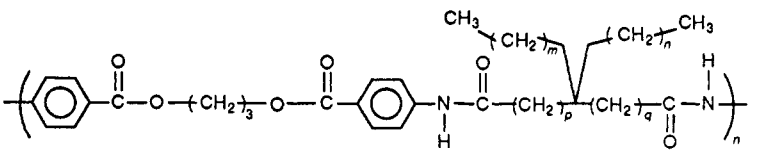

XIV

reproduced here) indicate that for all filler polymers used in this study, the dilute solution regime extends to beyond 2.5% concentration and that at 5% the polymers with the exception of the monodisperse oligomer are in the semidilute regime. Thus, the filler macromolecules are never in the concentrated regime when they are in the process of incorporation into the evolving "infinite" network gels.

Discussion

The information in the Results section strongly supports a fractal nature of the one-step rigid rodlike highly branched macromolecules in their pregel state and a significant retention of this nature in the gelled "infinite" network. Below, we shall briefly indicate the consistency of various results with the fractal model, first in the pregel and then in the postgel state.

(a) Fractal Nature of One-Step Rigid Rodlike Branched Macromolecules in Their Pregel State. In Figure 1 the increasing viscosity of the growing branched rigid macromolecules is plotted against time in a log–log plot. When the viscosity, or the reduced viscosity, is plotted against time on semilog paper, as was shown by Aharoni and Edwards,[20] the data points fall on one or two straight lines for all rigid or semirigid polymers. A flexible branched polymer required three straight lines to fit the pregel data. The above linearity of the growth kinetics of the branched rigid macromolecules in semilog plots is one of the criteria[32] for fractal growth. In Figure 2 the changes in viscosity are plotted on log–log paper against $(t_c - t)/t_c$ for three rigid systems and one flexible system. The slopes of the straight lines through the kinetic data points define a critical exponent for viscosity, k. For the rigid systems in their pregel state, k is 0.52, 0.76, and 0.97. For the flexible system $k = 1.85$. From the theoretical point of view, it does not matter much whether the viscosity or the intrinsic viscosity is used,[37] a fact that allows us to compare our results with the available literature (where s is occasionally used instead of k). Adam et al.[38] determined for a flexible system a value of $k = 0.78 \pm 0.04$, which is pretty close to a prediction by de Gennes[39] of $k \cong 0.75$, based on a three-dimensional percolation theory analogy to superconductivity. For epoxies, Martin et al.[40] obtained $k = 1.4 \pm 0.2$ and on silica gel $k = 1.5 \pm 0.2$ was obtained[41] by light scattering. Using the Rouse model approximation, the same percolation theory predicts $k = 1.3$ and with the Zimm model approximation a value of $k = 0$ is predicted.[37] A value of 1.7 for k was recently proposed by Hess and associates.[42] The theories are only reliable in simple clean experimental specifications, so we are only left with the knowledge that percolation theories predict a power dependence of the viscosity of the growing particles on polymerization time up to the gel point and that our systems are in qualitative agreement with these theories.

The intrinsic viscosity of our series 45X showed a dependence on M_w to the power of 0.419. The hydrodynamic radius dependence on M_w was found to follow a 0.487 power. According to Muthukumar,[43] at low frequencies in the dilute solution regime, the intrinsic viscosity of polymeric fractals is proportional to $M^{(d-D_f)/D_f}$ where d is the Euclidean dimensions, $d = 3$ in our case, and D_f is the fractal dimensionality. Our value of $[\eta] \propto M^{0.419}$ leads to

$$D_f = 2.11 \tag{8}$$

The radius of the growing fractal is related to its molecular weight as[43,44]

$$R^{D_f} \propto M \tag{9}$$

and our value of $R \propto M_w^{0.487}$ translates to $R^{2.053} \propto M_w$ with

$$D_f = 2.053 \tag{10}$$

It must be emphasized that our one-step highly branched rigid macromolecules were studied in pure DMAc and DMAc/5% LiCl, excellent solvents for these systems, so that there exists no similarity to Θ or poorer conditions occasioned in the case of linear polymers with such small power dependencies. A better perspective on the situation may be gained from Figure 11. Here are plotted on log–log paper hydrodynamic radii and radii of gyration of several polyamides against their M_w. All measurements were conducted in very good solvents for the respective polymers and no polyelectrolyte effects were present. Except for the results of series 45X and sample 59E in the present work, all data were taken from previous works by Aharoni and associates.[35,45-47] The rigid linear poly(*p*-benzanilide terephthalamide) (PBT) exhibited a dependence of the radius on M_w to the power of 0.81. The flexible linear polyamide poly(ε-caprolactam) shows a power dependence of 0.70, within the range of expectations for normal linear polymers in good solvent. The densely globular Boc-poly(α,ε-L-lysine), in which each monomer is trifunctional yet flexible, follows a power dependence of 0.35. This is very close to the power of 0.33 expected from dense spheres. Our fractals follow a dependence of 0.49. From the above it is obvious that, despite the fact that good solvent quality is maintained throughout, the decreased power dependence of the radii on M_w reflects the increased branching and relative compactness of the polyamides.

From Table III one gathers that the R_H for series 45X and 59E rest about halfway between the values calculated according to the free-draining and nondraining models. R_H is very much smaller than the Gaussian R_{Gg} or the R_{Gvisc} calculated from viscosity measurements as shown in ref 24. These results indicate that the highly branched rigid macromolecules are substantially porous on the scale of common organic solvent molecules. This conclusion is consistent with the values of D_f obtained from solution properties being substantially smaller than the corresponding values obtained, in Table V, from the slopes of the scattered X-ray intensity of the 1:2 pastes of 45X plotted against q. The above leads us to a picture of our one-step rigid highly branched macromolecules that, we believe, is consistent with all our observations. A two-dimensional representation of the one-step rigid macromolecules in their pregel state is shown in Figure 12. The macromolecule is characterized by a segment length of 38.5 Å between its stiff trifunctional branchpoints. In terms of series 45X or 59E, its number-average molecular weight is around 68 000. The small spherical macromolecule stands for Boc-poly(α,ε-L-lysine) of comparable molecular weight drawn on the same scale. The dark dot in the figure stands for a solvent molecule about 5 Å in diameter. The fractal nature of our one-step rigid macromolecules together with their porosity to small molecules is obvious. The compactness and impermeability to solvent of the Boc-poly(α,ε-L-lysine) globular molecules are now just as obvious. The high porosity to small molecules of our rigid fractals explains, we believe, the highly draining nature of these macromolecules in dilute solution and the porosity of the dried network to penetrants such as helium and pressurized mercury. Sample 45XB clearly demonstrates the open nature of our rigid fractals in dilute solution. From the volume inscribed by a hydrodynamic sphere with $R_H = 120$ Å and $M_w = 410\,000$, one calculates that the branched macromole-

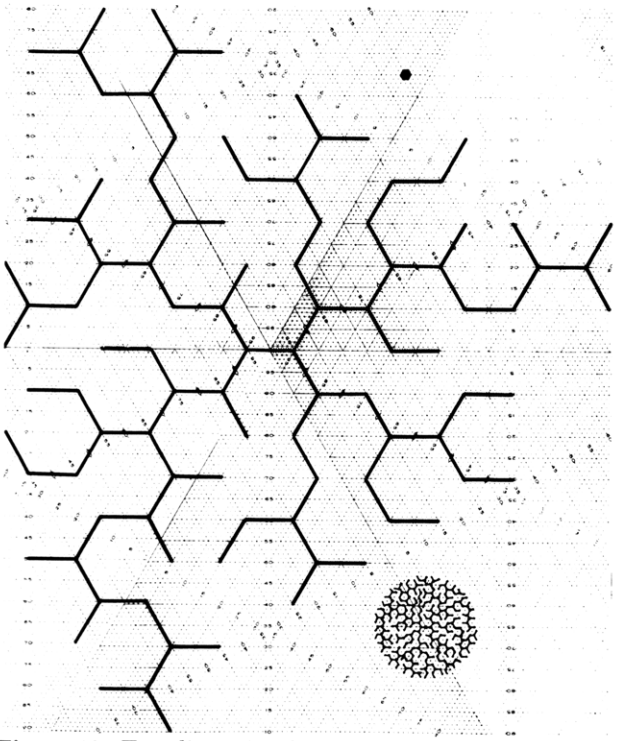

Figure 12. Two-dimensional representation of a rigid rodlike fractal with l_0 = 38.5 Å and stiff trifunctional branchpoints. The smaller sphere represents a Boc-poly(α,ϵ-L-lysine) macromolecule of the same molecular weight drawn to the same scale. The dot stands for a solvent molecule with a diameter of about 5 Å.

cule fills only 9.4% of a sphere with said radius. When M_n = 47 650 is used, the volume filled by the macromolecular matter reduces to 1.09%. Such low volume fractions are typical of all our rigid fractals.

It has been shown by Stockmayer[48] and Flory[6] that M_n of branched polymers increases slowly and more or less linearly, while M_w increases exponentially. In their case, intramolecular cyclization was neglected. Our rigid highly branched macromolecules appear as Cayley trees in which, due to branchpoint stiffness and segmental rigidity, intramolecular cyclization is highly unlikely. Therefore, our rigid fractals should follow the molecular weight distributions proposed by Stockmayer and Flory better than in the flexible systems that they were studying. Similar relationships were proposed to describe polymer fractals.[49] Proportionality (5) above gives us, hence, a reasonable approximation of the power law by which M_w changes as the condensation reaction progresses toward gelation.

The SAXS intensity data are, of course, most interesting. The slopes of $I(q)$ versus q for all the samples produce scattering exponents in the range 3–4. This implies that in the dry as well as in the solvent-swollen state we are looking at a "surface fractal" behavior where a power dependence of

$$I(q) \propto q^{-(6-D_s)}; \quad 2 \leq D_s < 3 \tag{11}$$

is expected. The value of D_s increases from exactly 2 for a smooth spherical surface separating two well-defined densities and approaches 3 for an extremely ramified and corrugated interface. Such an increase may be reflected in the changes in D_s observed in Table V, from closer to 2 for the dry samples to closer to 3 for the solvent-swollen ones.

The above SAXS results clearly reflect a fractal behavior of the one-step, rigid rodlike, highly branched macromolecules. This behavior is observed both in concentrated solution and in the dry state. These results are consistent with an increasing body of literature results of light, X-ray, and neutron scattering from fractal objects.[22,23,25–28,50–52] Importantly, the scattering results of sample 45XD indicate that the fractal nature of the system carries from the pregel to the postgel state in both dry and solvated states.

In this context it is worthwhile mentioning that the intensities of SAXS from Boc-poly(α,ϵ-L-lysine) measured by Aharoni and Murthy[46] produced slopes of 4 or more when plotted (uncorrected) on log–log paper against q. This clearly differentiates between the densely packed smooth-surfaced Boc-poly(α,ϵ-L-lysine) and the highly ramified and porous rigid fractals as in series 45X and 59.

The information obtained from light scattering and PCS experiments, SAXS intensity and segmental-tip iodine decoration, and titrations combine together to clearly reveal the fractal nature of our pregel, one-step, rigid rodlike, highly branched polymeric particles. The viscosity behavior of our systems, the kinetics of particle growth, and the direct observation of the dried systems by SEM all lend additional support to a fit with the polymeric fractal model.

(b) The Nature of One-Step Rigid Rodlike Networks in Their Postgel State and a Comparison with Two-Step Analogues. Thus far the growing rigid polymeric fractals were described either in a good low molecular weight (low-M) solvent or in a bone-dry state. Another way to probe the nature of the growing polymeric particles as they connect and form an "infinite" network is to incorporate in the reaction mixture un-cross-linkable high molecular weight (high-M) macromolecules, otherwise chemically and structurally similar to the network, and then study their effects on the formed network gel.

A glance, in Tables VI, VII, VIII, and IX indicates that within each one-step and two-step family the modulus of the neat gelled networks increases with the concentration of network material in the gel. This pattern holds for both the as-prepared gels, at $c = C_0$, and the DMAc-equilibrated ones, at $c = C$. The increase of the modulus, G, with network concentration is according to expectations, but the power dependence of G on c appears to be significantly smaller than the power of ~2.2 predicted in the literature[53–56] for flexible networks. We have insufficient data at present to obtain a better estimate of the power dependence. It appears, however, to be substantially smaller than was found by Aharoni and Edwards[20] for other gels of rigid networks. This small power dependence appears to be associated with rather high modulus values. That is, the modulus of the various neat networks starts rather high and does not decrease with dilution as much as it had dropped in the previous work.[20] The amount of soluble polymeric material extracted during equilibration of all neat networks in DMAc was much smaller in this study than the sol fraction in ref 20. We believe that both observations reflect the fact that in the present study the segmental length between branchpoints is usually shorter and that cross-links between fractals may be more numerous than in the previous work.[20] It may be that the slightly higher polymerization temperature in the present study contributed to higher cross-link efficiency. If this is indeed the case, then it is a clear indication of the sensitivity of the condensation reaction, and the resulting modulus and other gel properties, to apparently minor alterations in the reaction conditions before and after gelation took place.[57]

The most important observation one gleans from Tables

VI, VIII, and IX is that the presence of high-M filler macromolecules in one-step networks reduces the latter's modulus relative to the corresponding neat networks, and, conversely, the presence of the same filler molecules increases the modulus of comparable two-step networks. In all instances in this study, the modulus reduction was consistently observed in one-step rigid and flexible networks, with the filler macromolecules being rodlike, rigid X's or flexible. In fact, in the case of the one-step flexible networks, the presence of an equal amount of filler macromolecules reduced the modulus by orders of magnitude and, in one instance, even prevented gelation from taking place. This is a clear indication of the disruptive effect of the filler macromolecules on the ability to form macroscopic networks and on their homogeneity. Most importantly, however, the presence of comparable amounts of the monodisperse oligomer in the reaction medium of the one-step rigid network 48C, essentially chemically identical with the rodlike high-M filler macromolecules in 45D2, had practically no effect on the modulus of the as-prepared and DMAc-equilibrated gelled networks. The addition of the appropriate amounts of monomers to balance for the possible nonstoichiometry caused by the chain ends of high-M filler macromolecules, repeated several times, had no effect whatsoever on the properties of the resulting gels or on the reaction and gelation kinetics. Extensive previous work on these and similar systems[24,34,35,58-61] teaches us that no transamidation between the preformed filler and the growing network may take place under the reaction conditions used in this work. All the above leads us to conclude that the reduction in modulus is due to the size of the filler macromolecules. As long as there exists a reasonable compatibility between network and filler and no phase separation occurs, the large filler macromolecules induce a disruptive influence during the one-step formation of macroscopic networks and on their molecular level uniformity. The absence of an effect from the oligomer indicates, we believe, that by themselves filler–network interactions, such as dipolar interactions or hydrogen bonding directly between chains or through solvent molecules, cause no significant effect on the behavior of the filler-containing networks.

The reinforcing effect of the high-M macromolecular filler in the two-step rigid network gel, albeit small, indicates that when the network is formed from preexisting high-M chains with multiple cross-links per chain, it is insensitive to the existence of high-M filler in the reaction mixture: the high-M filler macromolecules do not disrupt significantly the formation of a network from preexisting high-M chains and a low-M cross-linking agent. In the case of flexible systems, theory predicts[16] that un-cross-linked macromolecules entangled with the cross-linked network increase the equilibrium modulus of the ensemble in proportion with the concentration of the chains between entanglements. Furthermore, it must be borne in mind that the above insensitivity to the presence of filler macromolecules may be substantially affected by the concentration of available branchpoints along each cross-linkable linear chain. In our case the distance between branchpoints along the rigid chains averaged to 33.9 Å, a rather high potential cross-link concentration.

The process of network formation must be understood in order to explain the difference in the response to the presence of filler macromolecules of the one-step and two-step networks and the relatively high modulus of the latter. Here, we refer back to Tables I and II, listing relevant members of series 45X and 59, respectively, Table VII comparing networks prepared from monomers and from fractals alone, and Figure 8 and its text in the Results section. In light of all these, and consistent with all other results in this study, we picture the evolving one-step rigid network as follows: polymeric multifunctional nuclei germinate at random throughout the reaction medium. The additon of monomers to these nuclei builds up highly branched polymeric fractals that gradually grow in number and size, concomitantly linking up and forming clusters. The linkup may occur directly between fractals or with the aid of monomeric or oligomeric species bridging them. Up to a length probably limited by the ability of the network to support the weight of the occluded solvent, the longer the segments the lower is the critical concentration C^*_0 above which an "infinite" network is formed. Gelation occurs when a sufficient number of fractals and fractal clusters come in contact with one another to form an "infinite" cluster in which contiguous fractals traverse the gel from one end to the other. Upon impingement, some covalent bonds are formed between fractals, and some segmental interpenetration ensues. Concurrently, fractals and clusters that are not an integral part of the network grow either interpenetrated with the network segments or nestled in and occluded by the "infinite" network.

The length of the rigid filler macromolecules is far greater than the size of the whole growing fractal, while the size of the rigid X's and flexible filler polymers are of the same order of magnitude as the fractals. It is possible that the thermodynamics of the solution of fractals plus fillers is such as to encourage a phase separation as the fractals increase in size. In that case, the filler macromolecules may be rejected by the growing fractals and be driven ahead of the growth fronts, away from the fractal cores. When two such fronts meet, the filler macromolecules remain stuck in between the two impinging fractals. By their mere presence they interfere with the creation of covalent bonds between the fractals, with segmental growth in the interfacial region and with interfacial segment interpenetration. We believe this to be the reason for the weakening of the one-step network by the presence of high-M filler molecules. Conversely, because the size of the monodisperse oligomers is smaller than that of the networks' segments, thermodynamics may not favor phase separation. The oligomers may then be easily accommodated within the intersegmental pores with their presence essentially unfelt and may cause no interference to the formation of covalent or other bonds.

The results discussed thus far are consistent with a fractal nature of the one-step rigid branched polymers in the pregel state. In our case, some aspects of the fractal nature are retained by the postgel network while others fade away and are overshadowed by the macroscopic behavior of the "infinite" network gel.

Morphologically, the two-step networks appear to be fundamentally different from the one-step ones. In the two-step case, the filler macromolecules in the reaction mixture are surrounded by cross-linkable macromolecules of comparable size. Once cross-linking occurs, the filler macromolecules remain trapped in their place. They are not being pushed ahead of any growth front simply because such fronts do not exist on the scale of the filler macromolecule. Furthermore, unlike the one-step case, a relatively very small number of cross-linking reactions are sufficient to create an "infinite" network in the second step of the two-step network. This also serves to immobilize the filler macromolecules. It is conceivable that the two-step network may be described in terms of

polymeric fractals, but we believe this is unlikely. If it does occur, then the size of the two-step fractals and the length of their arms during the cross-linking stage will be much larger than the corresponding sizes in the one-step systems. In fact, describing the two-step systems, especially the rigid rodlike ones, as cross-linked sheaflike seems to us more appropriate.

The nature of the two-step gelled networks is determined by their cross-linking reaction. In our case, we have long polymeric chains in concentrated or semiconcentrated solution, having many cross-linkable sites fixed along each chain at rather short distances. For example, there are about 50 such sites per each linear precursor chain of 51B. The cross-linking agent is difunctional and initially is uniformly distributed in solution. Because of the length of the original chains, several small cross-linking molecules may be concomitantly attached to each chain. When only one of these small molecules reacts at both its ends, a cross-link is formed. Because of the concentration during the formation of our two-step networks, it is not very favored that cross-links will preferentially concentrate along relatively short chain lengths to form small regions intensively cross-linked interspersed with regions of low or no cross-link density. We believe that some local variations in cross-link density may exist, but in the case of the two-step cross-linked sheaflike networks these variations are not expected to be large. Naturally, when the network is swollen in a good solvent, the dilute cross-link regions swell more than the dense cross-link regions, magnifying the difference between them.[62] Finally, it is important to recognize that, unlike our two-step systems, networks made exclusively by end-linking flexible chains are expected to pass through a fractal stage prior to gelation.[42]

Acknowledgment. We thank M. J. McFarland, E. Uyehara, M. F. Martin, and P. T. Connor for their help with various aspects of the experimental work. General discussions with Professors S. Krimm and G. Wegner and with Dr. J. S. Lin concerning SAXS are gratefully acknowledged. We also thank Dr. M. E. Cates for reading parts of an earlier version of this paper and alerting us to several references.

References and Notes

(1) Dušek, K.; Prins, W. *Adv. Polym. Sci.* **1969**, *6*, 1.
(2) Flory, P. J. *Discuss. Faraday Soc.* **1974**, *57*, 7.
(3) James, H. M.; Guth, E. *J. Chem. Phys.* **1943**, *11*, 455; **1947**, *15*, 669.
(4) James, H. M. *J. Chem. Phys.* **1947**, *15*, 651.
(5) Wall, F. T.; Flory, P. J. *J. Chem. Phys.* **1951**, *19*, 1435.
(6) Flory, P. J. *Principles of Polymer Chemistry*; Cornell University Press: Ithaca, NY, 1953; Chapters XI and XIII.
(7) Treloar, L. R. G. *The Physics of Rubber Elasticity*; Clarendon Press, Oxford, U.K., 1958.
(8) de Gennes, P.-G. *Scaling Concepts in Polymer Physics*; Cornell University Press: Ithaca, NY, 1979; Chapters V and VII.
(9) Daoud, M.; Bouchaud, E.; Jannink, G. *Macromolecules* **1986**, *19*, 1955.
(10) Duering, E.; Kantor, Y., in press.
(11) Kantor, Y.; Webman, I. *Phys. Rev. Lett.* **1984**, *52*, 1891.
(12) Bergman, D. J.; Kantor, Y. *Phys. Rev. Lett.* **1984**, *53*, 511.
(13) Alexander, S. *J. Phys. (Paris)* **1984**, *45*, 1939.
(14) Brown, W. D.; Ball, R. C. *J. Phys. A* **1985**, *18*, L517.
(15) Brown, W. D. Thesis, Cambridge University, Dec 1986.
(16) Doi, M.; Edwards, S. F. *The Theory of Polymer Dynamics*; Clarendon Press, Oxford, U.K., 1986; pp 188–217, 218–288.
(17) Vilgis, T. A.; Winter, H. H. *Colloid Poly. Sci.* **1988**, *266*, 494.
(18) Aharoni, S. M. *Macromolecules* **1982**, *15*, 1311.
(19) Aharoni, S. M.; Wertz, D. H. *J. Macromol. Sci.-Phys.* **1983**, *B22*, 129.
(20) Aharoni, S. M.; Edwards, S. F. *Macromolecules* **1989**, *22*, 3361.
(21) Yamazaki, N.; Matsumoto, M.; Higashi, F. *J. Polym. Sci. Polym. Chem. Ed.* **1975**, *13*, 1373.
(22) Martin, J. E.; Hurd, A. J. *J. Appl. Crystallogr.* **1987**, *20*, 61.
(23) Schmidt, P. W.; Hohr, A.; Neumann, H. B.; Kaiser, H.; Avnir, D.; Lin, J. S. *J. Chem. Phys.* **1989**, *90*, 5016.
(24) Ahroni, S. M. *Macromolecules* **1988**, *21*, 185.
(25) Schmidt, P. W. In *The Fractal Approach to Heterogeneous Chemistry*; Avnir, D., Ed.; Wiley: Chichester, 1989; pp 67–79.
(26) Quellet, Ch.; Eicke, H.-F.; Gehrke, R.; Sager, W. *Europhys. Lett.* **1989**, *9*, 293.
(27) Marignan, J.; Guizard, C.; Larbot, A. *Europhys. Lett.* **1989**, *8*, 691.
(28) Ogawa, T.; Miyashita, S.; Miyaji, H.; Suehiro, S.; Hayashi, H. *J. Chem. Phys.* **1989**, *90*, 2063.
(29) Mandelbrot, B. B. *The Fractal Geometry of Nature*; W. H. Freeman: New York, 1983; pp 10–11, 113, 162.
(30) Witten, T. A., Jr. *J. Polym. Sci. Polym. Symp.* **1985**, *73*, 7.
(31) Stanley, H. E.; Family, F.; Gould, H. *J. Polym. Sci. Polym. Symp.* **1985**, *73*, 19.
(32) Pope, E. J. A.; Mackenzie, J. D. *J. Non-Cryst. Solids* **1988**, *101*, 198.
(33) Wong, P.-Z. *Phys. Today* **Dec 1988**, 24–32.
(34) Aharoni, S. M. *Macromolecules* **1988**, *21*, 1941.
(35) Aharoni, S. M. *Macromolecules* **1987**, *20*, 2010.
(36) Aharoni, S. M.; Hatfield, G. R.; O'Brien, K. P. *Macromolecules* **1990**, *23*, 1330.
(37) Stauffer, D.; Coniglio, A.; Adam, M. *Adv. Polym. Sci.* **1982**, *44*, 103.
(38) Adam, M.; Delsanti, M.; Durand, D.; Hild, G.; Munch, J. P. *Pure Appl. Chem.* **1981**, *53*, 1489.
(39) deGennes, P. G. *C. R. Acad. Sci. Paris* **1978**, *286B*, 131.
(40) Martin, J. E.; Adolf, D.; Wilcoxon, J. P. *Phys. Rev. Lett.* **1988**, *61*, 2620.
(41) Martin, J. E.; Wilcoxon, J. P. *Phys. Rev. Lett.* **1988**, *61*, 373.
(42) Hess, W.; Vilgis, T. A.; Winter, H. H. *Macromolecules* **1988**, *21*, 2536.
(43) Muthukumar, M. *J. Chem. Phys.* **1985**, *83*, 3161.
(44) Cates, M. E. *J. Phys. (Paris)* **1985**, *46*, 1059.
(45) Aharoni, S. M.; Crosby, C. R., III; Walsh, E. K. *Macromolecules* **1982**, *15*, 1093.
(46) Aharoni, S. M.; Murthy, N. S. *Polym. Commun.* **1983**, *24*, 132.
(47) Aharoni, S. M.; Cilurso, F. G.; Hanrahan, J. M. *J. Appl. Polym. Sci.* **1985**, *30*, 2505.
(48) Stockmayer, W. H. *J. Chem. Phys.* **1944**, *12*, 125.
(49) Daoud, M.; Martin, J. E. In *The Fractal Approach to Heterogeneous Chemistry*; Avnir, D., Ed.; Wiley: Chichester, 1989; pp 109–130.
(50) Martin, J. E. *J. Appl. Cryst.* **1986**, *19*, 25.
(51) Wu, W.; Bauer, B. J.; Su, W. *Polymer* **1989**, *30*, 1384.
(52) Russo, P. S.; Chowdhury, A. H.; Mustafa, M. In *Materials Science and Engineering of Rigid Rod Polymers*; Adams, W. W., McLemore, D., Eds.; Materials Research Society: Pittsburgh, PA, 1989.
(53) Ferry, J. D. *Viscoelastic Properties of Polymers*; Wiley: New York, 1980; pp 224–263, 404–425, 529–544.
(54) Gottlieb, M.; Macosco, C. W.; Benjamin, G. S.; Meyers, K. O.; Merrill, E. W. *Macromolecules* **1981**, *14*, 1039.
(55) Edwards, S. F.; Vilgis, Th. *Rep. Prog. Phys.* **1988**, *51*, 243.
(56) Graessley, W. W. Adv. *Polym. Sci.* **1974**, *16*, 1.
(57) Brereton, M. G.; Filbrandt, M. *Polymer* **1985**, *26*, 1134.
(58) Aharoni, S. M. *J. Appl. Polym. Sci.* **1980**, *25*, 2891.
(59) Aharoni, S. M. *J. Polym. Sci., Polym. Phys. Ed.* **1981**, *19*, 281.
(60) Aharoni, S. M.; Hammond, W. B.; Szobota, J. S.; Masilamani, D. *J. Polym. Sci., Polym. Chem. Ed.* **1984**, *22*, 2579.
(61) Aharoni, S. M. *Macromolecules* **1987**, *20*, 877.
(62) Bastide, J.; Leibler, L. *Macromolecules* **1988**, *21*, 2647.